JCI The Journal of Clinical Investigation

Hepatocyte-specific suppression of ANGPTL4 improves obesity-associated diabetes and mitigates atherosclerosis in mice

Abhishek K. Singh, … , Yajaira Suárez, Carlos Fernandez-Hernando

J Clin Invest. 2021. https://doi.org/10.1172/JCI140989.

Research In-Press Preview Hepatology Metabolism

Graphical abstract

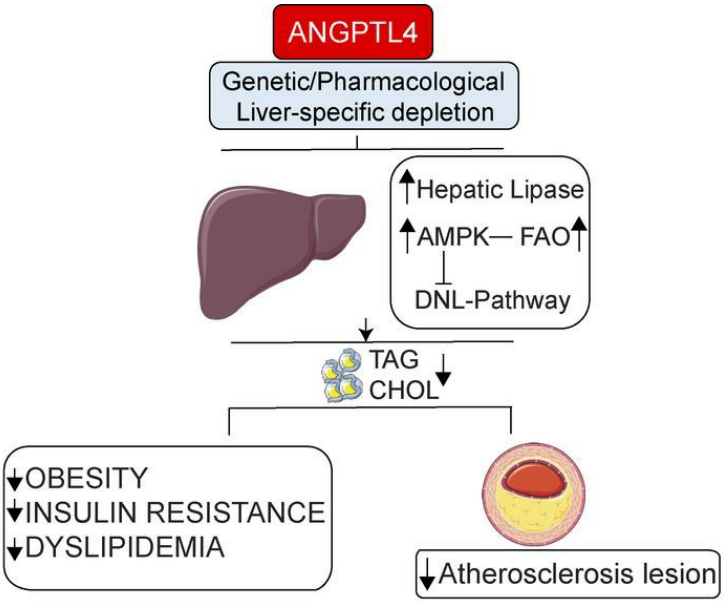

Hepatocyte-specific suppression of ANGPTL4 improves obesity-associated diabetes and mitigates atherosclerosis in mice

Abhishek K. Singh[1,2#], Balkrishna Chaube[1,2#], Xinbo Zhang[1,2], Jonathan Sun[1,2], Kathryn M Citrin[1,2,3], Alberto Canfrán-Duque[1,2], Binod Aryal[1,2], Noemi Rotllan[1,2], Luis Varela[2], Richard G. Lee[4], Tamas L Horvath[2], Nathan L. Price[1,2], Yajaira Suárez[1,2,5*] and Carlos Fernández-Hernando[1,2,5*]

[1]Vascular Biology and Therapeutics Program, Yale University School of Medicine, New Haven, Connecticut, 06520, USA.
[2]Integrative Cell Signaling and Neurobiology of Metabolism Program, Department of Comparative Medicine, Yale University School of Medicine, New Haven, Connecticut, 06520, USA.
[3]Department of Cellular and Molecular Physiology, Yale University School of Medicine, New Haven, Connecticut, 06520, USA.
[4]Cardiovascular Group, Antisense Drug Discovery, Ionis Pharmaceuticals, Carlsbad, CA, 92010, USA.
[5]Department of Pathology, Yale University School of Medicine, New Haven, Connecticut, 06520, USA.

#These authors contributed equally

[*]**Corresponding authors**:
Carlos Fernández-Hernando, PhD. 10 Amistad Street, Room 337c, New Haven, CT. 06520. Tel: (203) 737-*4615.* Fax: (203) 737-2290. Email: carlos.fernandez@yale.edu
Yajaira Suárez, PhD. 10 Amistad Street, Room 337c, New Haven, CT. 06520. Tel: (203) 737-8858. Fax: (203) 737-2290. Email: yajaira.suarez@yale.edu

Conflict of Interest: NA

ABSTRACT

Hepatic uptake and biosynthesis of fatty acids (FA), as well as the partitioning of FA into oxidative, storage, and secretory pathways are tightly regulated processes. Dysregulation of one or more of these processes can promote excess hepatic lipid accumulation, ultimately leading to systemic metabolic dysfunction. Angiopoietin-like-4 (ANGPTL4) is a secretory protein that inhibits lipoprotein lipase (LPL) and modulates triacylglycerol (TAG) homeostasis. To understand the role of ANGPTL4 in liver lipid metabolism under normal and high-fat fed conditions, we generated hepatocyte specific *Angptl4* mutant mice (*Hmut*). Using metabolic turnover studies, we demonstrate that hepatic *Angptl4* deficiency facilitates catabolism of TAG-rich lipoprotein (TRL) remnants in the liver via increased hepatic lipase (HL) activity, which results in a significant reduction in circulating TAG and cholesterol levels. Consequently, depletion of hepatocyte *Angptl4* protects against diet-induce obesity, glucose intolerance, liver steatosis, and atherogenesis. Mechanistically, we demonstrate that loss of *Angptl4* in hepatocytes promotes FA uptake which results in increased FA oxidation, ROS production, and AMPK activation. Finally, we demonstrate the utility of a targeted pharmacologic therapy that specifically inhibits *Angptl4* gene expression in the liver and protects against diet-induced obesity, dyslipidemia, glucose intolerance, and liver damage, which likely occurs via increased HL activity. Notably, this novel inhibition strategy does not cause any of the deleterious effects previously observed with neutralizing antibodies.

Key words: ANGPTL4, HL, AMPK, Diabetes, Atherosclerosis

INTRODUCTION

The liver is a central metabolic organ that is essential for regulating systemic glucose and lipid homeostasis (1, 2). Lipid homeostasis is maintained by the liver via a regulated balance between lipid acquisition (FA uptake and biosynthesis) and removal [FA oxidation (FAO) and very-low density lipoprotein (VLDL) secretion] (3-5). Dysregulation in these critical processes leads to the accumulation of excess triacylglycerol (TAG) in hepatocytes, resulting in the development of non-alcoholic fatty liver disease (NAFLD) and associated disorders such as hepatic insulin resistance (IR), type 2 diabetes (T2D) and atherosclerosis (5-10). The key pathological feature of NAFLD is the accumulation of intra-hepatic TAG, owing to increased flux of free FA (FFA) derived from lipolysis in adipose tissue (AT), dietary chylomicrons, and intrahepatic *de novo* lipogenesis (DNL) (5, 11). Lipoprotein lipase (LPL) plays a vital role in the homeostasis of lipid metabolism at the systemic level. However, the cellular mechanisms behind the regulation of lipid homeostasis in the liver still remains unclear.

ANGPTL4 is a multifaceted secreted protein that is highly expressed in metabolic tissues, most prominently in AT and liver (12-14). ANGPTL4 regulates many cellular and physiological functions, mainly via inhibiting LPL activity at the posttranslational level (15-20). Human genetics and clinical studies have emphatically demonstrated that mutations in the *ANGPTL4* gene (E40K) are associated with reduced plasma TAG and glucose levels (21-24). Importantly, the circulating level of ANGPTL4 is positively correlated with increased risk of cardiovascular disease (CVD) and T2D, along with obesity-associated diabetic phenotypes such as high BMI, fat mass, and altered glucose homeostasis (25). These observations indicate that ANGPTL4 is strongly implicated in the development of metabolic diseases in humans.

Early work on ANGPTL4 in rodents was performed using whole-body transgenic or knockout mouse models, thus limiting the ability to understand the specific role of ANGPTL4 in vital metabolic tissues. Therefore, some of the conclusions drawn from these studies have been

contradictory (13, 21, 26-30). A number of groups have shown that loss of *Angptl4* using knockout mouse models or monoclonal antibodies against ANGPTL4 results in mesenteric lymphadenopathy (inflammation of lymph nodes), chylous ascites, acute phase response, and severe gut inflammation upon high-fat diet (HFD) or western-type diet (WD) feeding, leading to metabolic complications and reduced survival (26, 31). In these studies, it is not clear whether these effects of *Angptl4* deficiency are LPL dependent or independent. This warrants a need for mouse models that are not affected by these confounding factors. Our recent work has demonstrated an essential role for adipose-derived ANGPTL4 in regulating lipid uptake and regulation of metabolic function by AT (32). We and others have observed that AT-specific *Angptl4* knockout (Ad-KO) mice displayed reduced circulating TAG levels, similar to what was observed in humans with a missense mutation in *ANGPTL4* (E40K variant) (32, 33). However, other factors identified in this study such as body weight and regulation of glucose homeostasis, were unaltered after chronic administration of HFD feeding (32). These findings suggest that ANGPTL4 in other tissues, such as the liver, could also play a key role in the regulation of whole-body metabolism. Moreover, the physiological roles of ANGPTL4 in liver metabolism are primarily unclear. Therefore, we generated a novel hepatocyte-specific mouse model (*Hmut*) in which exons 4-6 of *Angptl4* have been knocked out. Notably, we found that hepatocyte specific depletion of *Angptl4* prevents diet-induced obesity, reduces circulating TAGs, attenuates ectopic lipid accumulation, enhances insulin sensitivity and glucose tolerance and protects against the progression of atherosclerosis. Mechanistically, *Angptl4* deficiency in hepatocytes activates the hepatic lipase (HL) leading to an increase uptake of FA which results in Reactive Oxygen Species (ROS) production and activation of AMP-activated protein kinase (AMPK) in hepatocytes. Most importantly, therapeutic *Angptl4* expression inhibition of using N-acetylgalactosamine (GalNac)-conjugated antisense oligonucleotides (*Angptl4*-ASO) improves

metabolic homeostasis and prevents diet-induced obesity without eliciting any deleterious side-effects.

RESULTS

Hepatocyte-specific depletion of *Angptl4* alters systemic lipid metabolism

While the metabolic function of AT derived ANGPTL4 in regulating whole-body lipid and glucose metabolism have been recently elucidated, ANGPTL4 is also highly expressed in the human liver (**Figure 1A**), where its function is poorly understood. To understand the hepatocyte-specific role of ANGPTL4 on whole-body lipid and glucose metabolism, we generated conditional knockout mice, which were then bred with Albumin-Cre animals to specifically deplete the expression of *Angptl4* in hepatocytes (*Hmut*). The LoxP sites only flank exons 4-6 therefore, we analyzed the mRNA levels of the individual exons (1-7) of hepatic *Angptl4* through qRT-PCR. The expression of exons 1 to 3 and 7 was reduced by ~50%, whereas more than 95% reduction was observed for exons 4-6 in the liver of *Hmut* mice as compared to WT mice (**Figure 1B-C and Figure S1A**), with no compensatory increase in the expression of either ANGPTL3 or ANGPTL8 (**Figure S1B**). The expression of *Angptl4* was unaltered in WAT and BAT, reflecting the specific reduction of *Angptl4* in hepatocytes, with residual *Angptl4* mRNA present in Kupffer cells (KCs)/macrophages (**Figure S1C**). The purification of the different cellular populations was confirmed by measuring the expression of specific genes by qRT-PCR (**Figure S1D**). To assess whether hepatic *Angptl4* deficiency influences lipoprotein and glucose metabolism, we measured body weight and plasma levels of lipids and glucose in 2-month-old *Hmut* mice fed a chow diet (CD). Notably, we found a significant reduction in circulating TAGs, total cholesterol (TC), and HDL-C in *Hmut* mice (**Figure 1D**). We further confirmed these results by measuring TC and TAG in different lipoprotein fraction isolated by FPLC (**Figure 1E**). Fasting blood glucose

levels, body weight, and circulating NEFA levels were similar in both groups of mice (**Figure S1E-G**).

Absence of ANGPTL4 function in hepatocytes enhances hepatic lipid uptake

In order to understand how hepatocyte-derived ANGPTL4 regulates systemic lipid metabolism, we assessed possible causes of hypotriglyceridemia in *Hmut* mice. We reasoned that these effects could be due to either enhanced TRL (chylomicrons and VLDL) catabolism, reduction in hepatic VLDL production, or defective lipid absorption in the gut. To determine the impact of hepatocyte-specific suppression of *Angptl4* on the clearance of dietary TAGs (chylomicrons) in circulation, we administered mice with an intra-gastric gavage of olive oil and plasma TAGs and FFAs were measured at indicated time points post-gavage. We found that postprandial plasma levels of TAGs and FFAs were reduced in *Hmut* mice as compared to WT mice (**Figure 2A** and **B**). To identify the tissue(s) responsible for the enhanced lipid clearance, we analyzed lipid uptake using a [^{3}H]-oleate-labeled triolein tracer. Interestingly, *Hmut* mice displayed increased lipid uptake in the liver and accelerated clearance of circulating plasma lipid as compared to the WT control mice (**Figure 2C**). Next, we determined whether the accelerated clearance of TRL particles was a consequence of increased lipolytic activity. As such, we analyzed the HL and LPL activity in the plasma after heparin injection. Remarkably, *Hmut* mice had noticeably increased post-heparin plasma HL activity compared to WT mice (**Figure 2D**). To determine which liver cell type was influencing post-heparin plasma hepatic lipase activity, we measured HL activity in primary hepatocytes and KCs. Primary hepatocytes, but not KCs from *Hmut* mice had increased HL activity compared to hepatocytes and KCs isolated from WT mice (**Figure S2A**). Although the HL activity was higher in hepatocytes derived from *Hmut* mice, the expression levels of HL in both hepatocytes and KCs were similar in *Hmut* and WT cells (**Figure S2B**). Consistent with this finding, HL activity was markedly increased in the liver of *Hmut* as

compared to WT mice (**Figure S2C**). We then examined whether HL mediates TAG catabolism in *Hmut* mice. To achieve this, we treated *Hmut* mice with siRNA targeted against hepatic lipase (siHL *Hmut*) or a control antisense nucleotide (siC *Hmut*). Consistent with the above findings, suppression of HL (**Figure S2D**) normalized TAG levels in mice deficient in ANGPTL4 in hepatocytes (**Figure S2E**). In addition to differences in HL activity, we found a modest increase in post-heparin plasma LPL activity in *Hmut* compared to WT mice (**Figure 2E**). LPL activity was also significantly increased in the liver, but not in other tissues with high LPL expression, such as adipose tissues (WAT and BAT), heart, and muscle (**Figure S2F**). Similar to HL, LPL activity was significantly increased in hepatocytes, but not in KCs, of *Hmut* compared to WT mouse primary cells (**Figure S2G**), while affecting the expression of the enzyme was not affected (**Figure S2H**). Finally, we analyzed whether hepatic VLDL secretion and fat absorption also contributed to the reduction in circulating TAGs observed *Hmut* mice. As shown in **Figure 2F** and **G**, VLDL production and fat absorption were not affected by ANGPTL4 expression in hepatocytes. Together, these data indicate that hepatocyte specific loss of ANGPTL4 results in reduced circulating TAGs, likely due to enhanced hepatocyte HL and LPL-mediated lipolysis and clearance of TRL.

Lack of ANGPTL4 in the hepatocytes reduces body weight, fat mass, and hepatic neutral lipid accumulation

Elevated circulating TAGs might cause ectopic lipid deposition leading to insulin resistance (5, 7, 10, 34, 35). Therefore, we tested whether hepatocyte-specific depletion of ANGPTL4 could protect against diet-induced obesity and glucose intolerance after feeding mice a high-fat diet (HFD) for 16 weeks. We observed that *Hmut* mice gained significantly less weight than WT mice (**Figure 3A**). The difference in the body weight was independent of the food intake which was similar in both groups of mice (**Figure S3A**). This was accompanied by lower total

body fat mass, fat weight, and adipocyte cells size in the *Hmut* mice (**Figure 3B-D**). Similar to mice fed a CD, *Hmut* mice fed a HFD showed reduced plasma TAGs, TC, and HDL-C levels when compared to WT control mice (**Figure 3E**). These results were further confirmed by FPLC analysis (**Figure 3F**). Since alterations in body fat mass are often associated with changes in lipid accumulation in the liver (3, 36, 37), we determined neutral lipid content in the liver of *Hmut* and WT mice. As anticipated, we noticed a significant decrease in the liver weight of *Hmut* mice as compared to WT mice (**Figure 3G**). Oil-Red O and H&E staining of liver sections indicated reduced accumulation of neutral lipids in the liver of *Hmut* mice (**Figure 3H**), which was further confirmed by measuring TAG content in the liver (**Figure 3I**).

Elevated lipid deposition in the liver promotes the induction of hepatic inflammation (11). Therefore we investigated whether loss of *Angptl4* in hepatocytes influences hepatic inflammation under HFD fed conditions. We first analyzed the distribution of monocytes and KCs in the liver of mice challenged with HFD for 16 weeks. FACS analysis showed that lack of hepatocyte *Angptl4* reduced the proportion of monocytes in the liver, whereas we did not observe any differences in KCs between genotypes (**Figure S3B**). We also found a significant reduction in acute-phase response (APR) genes including serum amyloid A (*Saa*), haptoglobin (*Hp*) and lipocalin 2 (*Lcn2*) that arise from inflammation (38) in livers from *Hmut* compared to WT mice (**Figure S3C**). Moreover, circulating SAA levels were similar between both groups of mice (**Figure S3D)**. Consistent with these findings, *Hmut* mice did not show inflamed mesenteric lymph node (MLN) or Tuton giant cells during HFD feeding conditions (**Figure S3E**). Taken together, these data indicate that hepatic ANGPTL4 controls lipoprotein metabolism, and its absence improves the metabolic health of mice during pathophysiological conditions such as diet-induced obesity.

Loss of function of ANGPTL4 in hepatocytes improves glucose homeostasis and enhances insulin sensitivity in metabolic tissues

Recent studies on humans and mice have reported that loss of function of *ANGPTL4* is associated with improved glucose tolerance and insulin sensitivity (21, 27). Since diet-induced obesity is often accompanied by insulin resistance-linked glucose intolerance, we assessed the net functional outcome of hepatic *Angptl4* deficiency on systemic glucose metabolism during diet-induced obesity. We found that *Hmut* mice showed remarkably improved glucose tolerance and insulin sensitivity as compared to WT mice after 16 weeks of HFD feeding (**Figure 4A** and **B**). To further evaluate insulin sensitivity in different metabolic tissue(s), we assessed the levels of phosphorylated AKT (p-AKT) following insulin treatment. The results showed a markedly increased p-AKT/AKT ratio in skeletal muscle, AT, and liver of *Hmut* mice following intraperitoneal injection of insulin (**Figure 4C**), again suggesting enhanced insulin sensitivity in hepatocyte *Angptl4* deficient mice.

Reduced body weight and circulating lipids are associated with attenuated atherosclerosis in hypercholesterolemic mice

Human genetic studies have shown an association between loss of function variants of *ANGPTL4* and reduced risk of cardiovascular disease (24). Our results show that loss of *Angptl4* in hepatocytes significantly reduces circulating apoB-containing lipoproteins and improves glucose homeostasis, suggesting that suppression of *Angptl4* in hepatocytes might protect against the progression of atherosclerosis. To test this hypothesis, we injected *Hmut* and WT mice with an AAV8-PCSK9 adenoviral vector encoding a gain-of-function mutation in PCSK9 that degrades the LDL receptor (LDLR) and induces hyperlipidemia. These mice were then fed a Western-type diet for 16 weeks to induce atherosclerotic plaque formation (32). Consistent with the phenotype observed in HFD fed mice, we found that *Hmut* mice were resistant to weight

gain with no change in food intake upon WD feeding, which was reflected in reduced fat mass as compared to WT (**Figure 5A**; **Figure S4A** and **B**). While circulating HDL-C levels were unaltered, we observed a significant reduction in plasma TAGs and TC levels, as well as fasting blood glucose in *Hmut* mice 16 weeks after WD feeding (**Figure 5B**; **Figure S4C** and **D**). FPLC analysis revealed decreased TAG and cholesterol levels in VLDL fractions and cholesterol in IDL/LDL fractions of *Hmut* compared to *WT* mice (**Figure 5C**). Similar to what we observed in mice lacking *Angptl4* in adipose tissue (32), deficiency of *Angptl4* in hepatocytes also led to a significant reduction in atherogenesis when compared to WT littermates, as indicated by the reduced aortic root plaque area and diminished accumulation of neutral lipids as assessed by Oil-Red-O staining (**Figure 5D**). Furthermore, we also observed significantly decreased neutral lipid accumulation in the whole aorta of *Hmut* compared to WT mice (**Figure S4E).** The reduced lipid deposition in the aorta of *Hmut* mice was accompanied by a marked reduction in vascular inflammation, as shown by the significant decrease in macrophage accumulation in the lesions (**Figure 5E**). However, this effect was not accompanied by any significant difference in circulating blood leukocytes or proinflammatory monocytes ($Ly6C^{hi}$) (**Figure S4F**), nor plasma SAA levels between the groups (**Figure S4G**). Taken together, these results demonstrate that loss of function of ANGPTL4 in hepatocytes protects against diet-induced obesity and atherosclerosis.

Hepatocyte-specific loss of ANGPTL4 suppresses endogenous lipogenic pathway and promotes oxidative metabolism via AMPK activation

We next investigate the potential mechanisms by which loss of *Angptl4* in hepatocytes reduce hepatic lipid accumulation despite increased lipid uptake. To this end, we first analyzed the expression and activity of the main enzymes involved in *de novo* lipogenesis (DNL) including Acetyl CoA carboxylase (ACC), FA synthase (FASN), and HMG-CoA reductase (HMGCR) (39,

40). Notably, ACC phosphorylation, as well as FASN and HMGCR expression and activity were significantly reduced in the liver of *Hmut* mice as compared to *WT* mice fed a CD or HFD (**Figure 6A**-**C, Figure S5A** and **B**). In addition to the reduction in the activity of key enzymes involved in DNL, we also observed a marked increase in FA oxidation (FAO) in liver tissue isolated from *Hmut* mice (**Figure 6D**). We next studied the activation state of AMPK, which has been previously reported to be regulated by FA (41) and ANGPTL4 (42), and coordinates FA partitioning between oxidation and biosynthesis pathways by increasing FAO capacity and inhibiting DNL (43). Notably, we found a significant increase in AMPK phosphorylation (activated form) in the liver of *Hmut* mice as compared to WT (**Figure 6E**). To assess if enhanced lipid uptake mediated the AMPK activation in *ANGPTL4* depleted human hepatoma cells, we generated stable clones of HepG2 cells by lentiviral mediated transduction of specific shRNAs against *Angptl4*. ANGPTL4 mRNA and protein expression (measured in the cell culture media) were significantly reduced in *Angptl4* shRNA transduced cells compared to control cells (**Figure S6A** and **S6B**). To specificity of ANGPTL4 measurements were confirmed in HepG2 treated with hypoxia mimetics ($CoCl_2$), which induces the expression of ANGPTL4 and in human umbilical vein cells (HUVECs), known to express *ANGPTL4* (**Figure S6B**). Consistent with our *in vivo* findings, suppression of *ANGPTL4* expression resulted in enhanced FA uptake in HepG2 cells (**Figure 7A**). To determine the contribution of HL to the lipid uptake and FA-mediated AMPK activation observed in *ANGPTL4* silenced HepG2 cells, we silenced *HL* (**Figure S6C**) and analyzed lipid uptake and AMPK activation. We found that the increased lipid uptake and AMPK phosphorylation, in response to reduced expression of *ANGPTL4* (shANGPTL4), were diminished upon silencing of *HL* (**Figure 7B** and **C**). These results suggest that increased HL activity mediates AMPK activation, likely due to enhanced lipid uptake.

Previous work has implicated ROS in the activation of AMPK (44, 45), and increased FAO promotes ROS generation (46). Therefore, we next assessed if *ANGPTL4* silencing increases

ROS production and AMPK activation in HepG2 cells. As shown in **Figure 7D**, ANGPTL4 suppression in HepG2 cells results in a significant increase in dihydroethidium (DHE) staining, indicating higher ROS levels. This effect on ROS levels, was attenuated when cells were treated with etoximir (**Figure 7D**), a FAO inhibitor (47). Thus suggesting that elevated ROS were a consequence of increased FAO. To determine whether the increased FAO observed in ANGPTL4 depleted cells was mediated by HL-regulated TAG lipolysis and FA uptake, we silenced *HL* in shC and shAngptl4 transduced cells. The results showed that genetic silencing of *HL* attenuates ROS production in cells lacking ANGPTL4 (**Figure 7E**), suggesting that enhanced FA uptake in absence of ANGPTL4 contributes to the generation of ROS. Next, we asked whether the increase in ROS levels may serve to further promote sustained AMPK activation. To this end, we treated control and *ANGPTL4*-deficient cells with N-acetyl-l-cysteine (NAC), which is commonly used to scavenge ROS, and Compound C (CompC), an inhibitor of AMPK. NAC treatment attenuated the increased ROS accumulation, AMPK phosphorylation, and FAO observed in ANGPTL4 depleted cells (**Figure 7F**-**H**). Most importantly, direct inhibition of AMPK blunted the increased FAO in HepG2 cells transduced with shAngptl4 (**Figure 7F** and **H**), which correlated with a significant reduction in FAO associated genes (**Figure S6D**). In contrast, the expression of *ACC*, *FASN* and *HMGCR* was downregulated in *ANGPTL4*-deficient hepatoma cells, which was normalized by with either CompC or NAC (**Figure S6E**). The suppression of the lipid biosynthetic genes was associated with diminished mTORC1 mediated SREBP1 activation (**Figure S6F**). These findings suggest that the negative regulation of mTORC by AMPK (48, 49) controls the expression of genes associated with lipid biosynthesis. Indeed, inhibition of AMPK or suppression of ROS using CompC and NAC, respectively attenuates this effect.

We next assessed whether ROS mediated AMPK activation is involved in mediating the effects of *Angptl4* deficiency on hepatic FA metabolism *in vivo*. To this end, we administered

Hmut mice with either CompC or NAC. Treatment with NAC reduced ROS levels in primary hepatocytes isolated from *Hmut* mice (**Figure 8A** and **B**). Most importantly, CompC or NAC suppressed the increase in AMPK and ACC phosphorylation, FAO, and the expression of genes involved in FAO (e.g. *Pgc-1*α, *Cpt1a*, *Crot*, and *Hadhb*) observed in *Hmut* mice (**Figure 8C-E**). In contrast, the downregulation of DNL enzymes acitivity and the mRNA levels of *Acc*, *Fasn* and *Hmgcr* found in primary hepatocytes from *Hmut* mice was significantly attenuated after CompC or NAC treatment (**Figure 8F-H**). Taken together, these results suggest that increased lipase-mediated FA uptake in response to the absence of ANGPTL4 function in hepatocytes causes a compensatory increase in AMPK activation and FAO, which leads to increased ROS production further propmoting sustained activation of AMPK (**Figure 8I**).

Finally, we studied whether excess lipid uptake in the hepatocytes owing to the elevated HL activity in the absence of ANGPTL4 might promote endoplasmic reticulum (ER) stress response which could lead to increase ROS production (50) and insulin resistance (51, 52). Interestingly, we observed decreased levels of some of the key ER stress markers such as XBP1 and CHOP in the liver of *Hmut* as compared to *WT* mice (**Figure S7A** and **B**). Furthermore, we did not observe significant effect on unfolded protein response (UPR)-mediated activation of endoplasmic reticulum oxidoreductin-1 (ERO1) and mitochondrial Ca^{2+} levels (**Figure S7B** and **C**) which affects mitochondrial membrane potential and elevates mitochondrial ROS production (50). These data suggest that the elevated ROS under *ANGPTL4* deficiency is independent of lipid loading-mediated ER stress/UPR.

GalNac-conjugated *Angptl4* ASO reduces circulating TAGs, improves glucose tolerance and protects against diet-induced obesity

Human genetic studies have shown that loss of function mutations in the *ANGPTL4* locus are associated with reduced T2D and risk of CVD (21, 22, 25). Given the beneficial metabolic

effects observed in mice lacking *Angptl4* in hepatocytes, we evaluated whether a targeted inhibition of *Angptl4* expression in the liver improves metabolic homeostasis. To this end, we treated mice with GalNac conjugated ASO against *Angptl4*. These constructs have a high-affinity for the hepatocyte-specific asialoglycoprotein receptor, therefore its conjugation allows specific inhibition of a target gene in the liver (53). Ten-week-old male C57BL6 mice were administered with GalNac-conjugated *Angptl4* ASOs (*Angptl4* ASO) or GalNac-control ASOs (Ctrl ASO) via retro-orbital injection once a week for six weeks under CD fed conditions (**Figure 9A**). Six weeks after the treatment, *Angptl4* mRNA levels were markedly decreased in the liver without affecting *Angptl4* expression in KCs and AT (**Figure 9B** and **Figure S8A**). Similar to the results observed in the hepatocyte specific *Angptl4* deficient mice, administration of *Angptl4* ASO resulted in decreased plasma TAGs, TC, HDL-C and glucose levels (**Figure 9C** and **D**). These findings were further confirmed by FPLC analysis (**Figure S8B**). Similar to *Hmut* mice fed a CD, *Angptl4* ASO treatment also resulted in elevated HL and LPL activity without affecting body weight (**Figure S8C-E**).

To further determine whether therapeutic *Angptl*4 expression inhibition of in the liver attenuates HFD-induced obesity and insulin resistance, mice were fed a HFD for 4 weeks followed by administration of *Angptl4* ASO for six weeks along with HFD feeding (**Figure 9E**). *Angptl4* ASO treatment significantly protected against body weight gain and increase in fat mass in response to HFD feeding (**Figure 9F**). In addition, *Angptl4* inhbition resulted in decreased circulating TAGs compared to Ctrl ASO mice (**Figure 9G** and **Figure S8F**). Plasma TC levels were slightly decreased in *AngptL4* ASO treated mice and HDL-C were similar in both groups of mice (**Figure 9G** and **Figure S8F**). Moreover, we observed a significant improvement in glucose tolerance and insulin sensitivity in mice administered *Angptl4* ASO as compared to Ctrl ASO (**Figure 9H** and **I**).

Since global *Angptl4* deficiency in mice leads to severe systemic metabolic and inflammatory complications when fed for ~10 weeks on HFD diet (26), we next assessed whether hepatocyte-specific inhibition of *Angptl4* using *Angptl4* ASO improves whole-body metabolic homeostasis without causing any deleterious effects. In contrast to complete loss of *Angptl4*, *Angptl4* ASO therapy does not influence gut inflammation, chylous ascites, MLN inflammation (presence of Touton giant cells and *Cxcl1*, *Ptgs2* and *Ccr1* expression), or circulating leukocytes levels (**Figure 9J**; **Figure S9A-D**). These data indicate that the reduction in body weight of *Angptl4* ASO treated mice (**Figure S9E**) was not due to a reduction of food intake (**Figure S9F**), nor inflammation of the gut or MLN. We also found a significant reduction in the liver weight and hepatic TAG levels in mice treated with *Angptl4* ASO (**Figure S9G** and **H**). Additionally, *Angptl4* ASO treated mice were protected against HFD induced liver damage, as evidenced by lower plasma levels of hepatic enzymes alanine aminotransferase (ALT) and aspartate aminotransferase (AST) as well as reduced circulating liver-derived acute phase protein SAA (**Figure 9K; Figure S9I**). Together, these data indicate that specific silencing of *Angptl4* in the liver using GalNac-conjugated ASOs recapitulates the beneficial effects observed in *Hmut* mice in both physiological as well as pathological conditions. Most importantly, hepatic ANGPTL4 silencing was able to restore metabolic function in animals that were already obese, suggesting that this therapeutic approach may provide a viable treatment option for obesity related metabolic disorders, including T2D and cardiovascular disease.

Inhibition of the expression of hepatocyte derived *Angptl*4 increases energy expenditure.

Mice with hepatocyte-specific loss of *Angptl4* are protected against diet-induced obesity. To elucidate how hepatocyte-specific expression inhibition of *Angptl4* improves whole-body energy metabolism under HFD fed conditions (after six-week treatment of *Angptl4* ASO during HFD feeding) we performed metabolic cage analyses. We observed an increase in oxygen

consumption, CO_2 production, energy expenditure (EE) and locomotor activity in *Angptl4* ASO treated mice compared to control ASO treated mice during dark and light cycles (**Figure 10A-D** and **Figure S10A**). However, food consumption and respiratory exchange ratio (RER) remained unchanged (**Figure 10E** and **Figure S10B**). Similarly, gut lipid (energy) absorption was not different between the groups (**Figure S10C**). Together, these findings suggest that hepatocyte-specific deficiency of *Angptl4* reduces diet-induced obesity, likely by increasing energy expenditure.

DISCUSSION

Elevated circulating TAGs lead to elevated risk of cardiometabolic diseases such as obesity, T2D, and CVD, which are associated with increased adiposity, fatty liver, and insulin resistance (21-23, 25, 54, 55). Human studies have shown a positive correlation between ANGPTL4 function and body mass index (BMI), fat mass, glucose intolerance, insulin resistance, and circulating lipids (25, 56, 57). These observations implicate ANGPTL4 as a mediator, and potential therapeutic target for treating dyslipidemia associated diseases. However, the exact function of ANGPTL4 in regulating whole-body lipid and glucose metabolism has not been is fully elucidated due to the lack of tissue specific knockout mouse models. This is especially relevant because severe systemic metabolic complications (i.e., Ascites, MLN and gut inflammation) confound the researcher's ability to investigate the beneficial functions of *Angptl4* in whole-body knockout mice upon HFD/WD feeding (26, 31). Since ANGPTL4 is highly expressed in the liver and AT of both humans and mice, we generated *Angptl4* deficient mouse models specific to these tissues. Our previous work demonstrated that adipose-specific *Angptl4* knockout (Ad-KO) mice exhibit improved plasma lipid profiles and insulin sensitivity, but no difference in body weight was observed between Ad-KO and WT mice during prolonged HFD feeding (32). Similar results were recently reported by Davies laboratory (33). As the overall

impact on systemic metabolism was not as profound as expected, we hypothesized that ANGPTL4 derived from another vital metabolic organ involved in lipid homeostasis might be responsible for the effects on whole-body lipid and glucose metabolism observed in human studies. Interestingly, the ablation of hepatic ANGPTL4 resulted in decreased body weight, plasma lipids (TAGs and TC), and hepatic steatosis, as well as improved glucose tolerance and insulin sensitivity after 16-weeks of HFD feeding. The effects observed in *Hmut* mice were more pronounced than those found in Ad-KO mice, indicating that the deficiency of ANGPTL4 in hepatocytes has major consequences on systemic lipid and glucose metabolism.

Since *Hmut* mice were generated via removal of exons 4-6, therefore, it is possible that truncated protein might still be produced. However, truncated protein might not be functional, as we observed a significant increase in HL and LPL activity both in the liver (primary hepatocytes) and post heparin plasma in the *Hmut* mice. In agreement with this observation, the Kersten group have recently reported that *Angptl4* hypomorph mice (same mouse model that the one we have used in this study) have similar circulating TAG levels as the global *Angptl4* deficient mice (58), suggesting that the ANGPTL4 truncated isoform does not affect LPL function. Moreover, Davies and colleagues have shown that the overexpression of an *Angptl4* construct similar to the one used to develop our mouse model does not affect LPL activity (33). Together, these studies demonstrate that the potential truncated ANGPTL4 protein generated from this transcript is not functional and does not influence LPL activity in mice.

The improved circulating lipids in hepatocyte-specific *Angptl4* mutant mice was accompanied by accelerated TRL-remnant catabolism. We observed increased plasma TAG clearance and enhanced HL activity in *Hmut* mice. To confirm that ANGPTL4 regulates HL activity, we silenced HL in *Hmut* mice using siRNA and showed a reversal of the plasma lipid levels, indicating that ability of ANGPTL4 to decrease circulating TAG levels is mediated via HL-dependent TAG lipolysis in our model. These results are in line with a previous report by

Lichtenstein and colleagues showing the suppression of post-heparin HL activity in adipose tissue-specific overexpressing *Angptl4* mice (12). In contrast, other studies have shown that *Angptl4* knockout mice and liver-specific overexpression of *Angptl4* did not influence HL activity (28, 59). The reason for the discrepancy among these studies is unclear, but may be related to the differences in the mouse models used (magnitude of ANGPTL4 expression and overexpression of mouse *Angptl4 vs* human *ANGPTL4*) and the sensitivity of the assay used for measuring plasma HL activity. Increased LPL activity in hepatocytes might also contribute to the reduced circulating TAGs due to decreased levels of VLDL, consistent with existing data from previous studies (12). Nevertheless, our data suggest that much of the systemic changes in lipid homeostasis in the absence of functional hepatic ANGPTL4 may be mediated by increased HL activity.

In addition to acting as a lipolytic enzyme, HL facilitates the uptake of chylomicrons and VLDL remnants by hepatocyte cell surface receptors, thus contributing to the lowering of circulating lipids (60, 61). Comparison of FPLC plasma lipoprotein cholesterol profiles (IDL/LDL-fraction) in atherogenic mice further indicates that the protective impact of hepatic depletion of ANGPTL4 involves the contribution of elevated HL activity. Increased HL activity could facilitate the uptake of TRL-remnants in hepatocytes to prevent the accumulation of atherogenic lipoproteins in atherosclerotic plaques (62). As such, genetic ablation of ANGPTL4 in hepatocytes markedly reduces circulating pro-atherogenic lipoproteins and attenuates the progression of atherosclerosis. We also noticed that the depletion of hepatic ANGPTL4 leads to AMPK-mediated suppression of HMGCR expression and activity. Therefore, we believe that the suppressed activity of HMGCR in *Hmut* mice might contribute to reduced atherogenic lipoproteins and cholesterol in the plasma. These data suggest that hepatic ANGPTL4 may have a unique role in regulating both HL and HMGCR activity during the progression of atherosclerosis.

In contrast to our prior work in adipose deficient *Angptl4* mice (32), we found that loss of hepatic ANGPTL4 protects against body weight gain upon HFD/WD feeding, mainly by reducing visceral fat mass and liver weight, without affecting food intake. Metabolic analyses suggest that depletion of hepatic ANGPTL4 resulted in substantially higher energy expenditure without affecting food intake, which supports the reduction of fat mass for maintaining the balance of whole-body energy metabolism. Moreover, the reduction in fat mass and size of adipocytes in *Hmut* mice may be due in part to the accelerated hydrolysis of TRL remnants and increased FA uptake in the liver, thus leading to decreased circulating TAGs and reduced lipid storage in AT. The role of ANGPTL4 in mouse body weight regulation under both physiological and pathophysiological conditions has been controversial (13, 21, 28, 32). The reasons for these discrepancies are unknown, but may be due to the inactivation of different exons of the N-terminus of ANGPTL4 between knockout models, different types of diet, and the magnitude of overexpression. Structure-function analysis of ANGPTL4 from various knockout models through protein crystallography or Cryo-EM may eventually justify these discordant findings.

Despite increased lipid uptake in the liver, we found a marked reduction in the intrahepatic lipid accumulation in *Hmut* mice. We also observed a concomitant increase in the rate of FAO in the liver, thus suggesting that excess fat taken up by the liver is dissipated through enhanced β-oxidation via activation of AMPK upon *Angptl4* deletion. AMPK is known to increase FAO and suppresses DNL by inhibiting ACC. Thus, heightened AMPK activity may be one of the mechanisms by which hepatic deletion of *Angptl4* improves metabolic function following HFD-induced obesity. This hypothesis is supported by recent studies on the overexpression of AMPK in the mouse liver (63, 64). Moreover, ANGPTL4 has been reported to regulate AMPK activity to modulate metabolic homeostasis (42). Data from these studies indicate that activation of AMPK in the liver decreases lipid deposition not only in the liver, but also in the AT. Thus, improvements in whole-body glucose homeostasis and insulin action in *Hmut* mice upon

prolonged HFD feeding are likely downstream of the marked reduction in lipid accumulation in the liver and adipose tissue.

In the present study, we demonstrate a novel mechanism by which ANGPTL4 regulates lipid homeostasis via a mechanism involving HL/ROS/AMPK axis (**Figure 8I**). This mechanism is supported by several lines of evidence. Firstly, increased lipase-mediated lipid uptake causes a compensatory increase in AMPK-mediated FAO (46). It is well established that AMPK is critical to the adaptive response of FA metabolism (65-67). Activated AMPK upregulates β-oxidation of FA by inhibiting ACC. Dysregulation of AMPK signaling is associated with a diminished capacity to regulate FA oxidation to FA availability, leading to lipid accumulation and insulin resistance. Our study shows a prominent role of AMPK in controlling FA metabolism in hepatocytes lacking ANGPTL4. In addition, previous studies suggest that elevated FA or lipid accumulation can activate AMPK via CD36-dependent activation of LKB1 and independent of cellular energy state (65-67). Our data also indicate that suppression of HL expression in hepatocytes lacking *Angptl4* attenuates the lipid uptake which is correlated with decrease AMPK activation and ROS generation. These findings suggest that the HL-mediated increase in FA uptake in hepatocytes lacking *Angptl4*, is required for adaptive activation of AMPK. However, persistent activation of AMPK is required to fully promote the beneficial metabolic effects observed with hepatocyte-specific loss of ANGPTL4. It is known that FAO promotes ROS generation, and ROS is a well-known regulator of AMPK. Thus, ROS seems to play a key role in continuality activating AMPK in the hepatocytes facilitating sustained FAO. Moreover, our data indicate that suppression of ROS-mediated AMPK activation is sufficient to reverse the metabolic phenotype observed in *Hmut* mice. Our data demonstrate that FAO is a source of ROS in ANGPTL4-deficient cells and elevated ROS are required for maintaining AMPK-dependent high rate of FAO (**Figure 8I**). ROS at a physiological level play a key role in the cellular signaling as well as in the regulation of several metabolic pathways (68). Our data suggest that reducing ROS with the scavenger NAC

not only suppressed activation of AMPK but also reversed changes in hepatic lipid metabolism in *Hmut* mice. These observations suggest that ROS is a key mediator underlying the inverse relationship between AMPK and ANGPTL4.

In the recent years, studies have shown that ANGPTL4 act as potent metabolic regulator and is strongly associated with various metabolic disorders. Attempts to inhibit ANGPTL4 using a neutralizing antibody in humanized mice and non-human primates were confounded by severe systemic metabolic abnormalities (22). Our data from *Hmut* mice support the hypothesis that hepatocyte-specific suppression of *Angptl4* might have therapeutic potential in metabolic diseases. Therefore, we evaluated whether therapeutic inhibition of *Angptl4* expression in the liver recapitulates the beneficial metabolic phenotype afforded by genetic depletion of ANGPL4 in hepatocytes. Interestingly, *Angptl4* ASO treated mice were ameliorated from HFD-feeding-induced obesity and had improved circulating TAGs, glucose tolerance, and insulin sensitivity. Conclusively, this study reveals that *Angptl4*-ASO mediated inhibition of hepatic *Angptl4* consistently replicates most aspects of the obesity-resistant phenotype observed in *Hmut* mice. Most importantly, mice treated with *Angptl4* ASO did not exhibit any of the systemic metabolic abnormalities observed in previous studies. Thus, this study provides a strong rationale for following the development of liver-specific ANGPTL4 therapeutic agents for treating of cardiometabolic diseases.

Limitations

While the findings of this study, along with our prior work has considerably improved our understanding of how ANGPTL4 in vital metabolic organs impacts the ability to maintain metabolic homeostasis, there are still important questions and caveats that will need to be addressed in the future. Most importantly, ANGPTL4 is a secreted protein, and our current work has been unable to determine how the deficiency in the liver or AT precisely influences

circulating levels of ANGPTL4 and what impact this may have on lipid metabolism in other tissues. To explore this further, a specific and reliable antibody against mouse ANGPTL4 needs to be generated to measure serum ANGPTL4 levels. In addition, we used a pharmacological inhibitor of AMPK, CompC, which might have off-target effects. Therefore, a genetic approach to silence AMPK in the liver would be a useful secondary approach. Lastly, in response to the loss of function of ANGPTL4 in the hepatocytes, elevated HL activity was associated with decreased plasma HDL-C under physiological conditions. However, this relationship was not apparent under pathophysiological situations such as obesity and diabetes, thus further mechanistic investigation is needed to elucidate the relationship between HL and HDL-C during lipid overload conditions.

MATERIALS AND METHODS

Detailed information on experimental procedures and reagents is provided Supplemental Methods.

Animal studies

Generation of hepatocyte-specific *Angptl4*-deficient mice. Mice bearing a loxP-flanked *Angptl4* allele (*ANGPTL4*$^{loxP/loxP}$ mice) were generated as described previously (32). Hepatocyte-specific *Angptl4*–deficient mice (Albumin-Cre; *Angptl4*$^{loxP/loxP}$, *Hmut*) were generated by breeding albumin-Cre; *Angptl4*$^{loxP/+}$ mice with *Angptl4*$^{loxP/+}$ mice. All mouse strains were in the BL6 genetic background. *Hmut* mice were verified recombination within the *Angptl4* gene in the liver by PCR using Cre primers and primers flanking the 5′ homology arm of the *Angptl4* gene and LoxP sites from the tail-extracted DNA. All experimental mice were housed in a barrier animal facility with a constant temperature and humidity in a 12-hour dark/light cycle while water and food were provided *ad labium*. All mice (n=3-5 per cage) were fed with a standard chow diet (CD) for 8 weeks after that switched to an HFD (60% calories from fat; Research Diets D12492) for 1–16 weeks. To assess whether ANGPTL4 regulates plasma lipid levels through a hepatic lipase mediated pathway, Hmut mice were injected with locked nucleic acid (LNA) conjugated siRNA against HL through retro-orbital route at a dose of 20 mg/kg twice a week for two weeks. For atherosclerosis studies, mice (8-week-old, n=3-5 per cage) were administered with a single retro-orbital injection of recombinant adeno-associated virus (AAV, containing 1.0×10^{11} genome copies) encoding PCSK9 (AAV8.ApoEHCR-hAAT.D377Y-mPCK9.bGH) to induce hyperlipidemia (32). Two weeks' post-injection, atherosclerosis was induced by feeding the mice with high cholesterol, western diet (WD) containing 1.25% cholesterol (D12108, Research Diets). Body weight and food intake were measured every week of HFD and WD fed mice.

For liver-specific *Angptl4* antisense oligonucleotide (ASO) studies, mice, at ten weeks of age, were injected with GalNac-control ASO (Ctrl ASO) or GalNac conjugate *Angptl4* ASO (*Angptl4*

ASO) (the combination of two ASOs) through retro-orbital rout at a dose of 25mg/kg/week for six weeks. ASO sequences used in this study were as follows: Angptl4 ASO (1) 5'-AGCTGTAGCAGCCCGT-3' (2) 5'-ATATGACTGAGTCCGC-3' and control ASO 5'-GGCCAATACGCCGTCA-3'. ASOs were dissolved in PBS for the mice experiments. During the GalNac conjugated *Angptl4* ASO treatment, mice were fed with CD. To assess the therapeutic effect of GalN-ASO in obese mice, mice were fed a HFD for 4 weeks and were treated with GalNac-cntr ASO or GalNac-*Angptl4* ASO (25mg/kg) by retro-orbital injections weekly for the 10 weeks.

Statistics

The mouse sample size for each study was based on literature documentation of similar well-characterized experiments. The number of mice used in each study is listed in the figure legends. In vitro experiments were regularly repeated at least three times unless otherwise noted. No inclusion or exclusion criteria were used, and studies were not blinded to investigators or formally randomized. Data are expressed as average ± SEM. Statistical differences were measured using an unpaired 2-sided Student's t-test, or 1-way or 2-way ANOVA with Bonferroni's correction for multiple comparisons. Normality was tested using the Kolmogorov-Smirnov test. A nonparametric test (Mann-Whitney) was used when the data did not pass the normality test. A value of $P \leq 0.05$ was considered statistically significant. Data analysis was performed using GraphPad Prism software version 7.

Study approval

Animal experiments were conducted under the ethical guidelines and protocols approved by IACUC at Yale University School of Medicine (Animal protocol #2019-11577).

AUTHOR CONTRIBUTIONS

AKS, BC, YS and CF-H conceived and designed the study and wrote the manuscript. AKS, BC, ACD, XZ, BA, JS, KC, LV and NR performed experiments and analyzed data. NLP, KC and TLH analyzed data and edited the manuscript.

ACKNOWLEDGEMENTS

This work was supported at least in part by grants from the National Institutes of Health (R35HL135820 to CF-H and 5F32DK10348902 to NP), the American Heart Association (16EIA27550005 to CF-H, 20TPA35490202 to YS and 17SDG33110002 to NR), the American Diabetes Association (1-16-PMF-002 to AC-D).

REFERENCES

1. Bechmann LP, Hannivoort RA, Gerken G, Hotamisligil GS, Trauner M, and Canbay A. The interaction of hepatic lipid and glucose metabolism in liver diseases. *J Hepatol.* 2012;56(4):952-64.
2. Petersen MC, Vatner DF, and Shulman GI. Regulation of hepatic glucose metabolism in health and disease. *Nat Rev Endocrinol.* 2017;13(10):572-87.
3. Fabbrini E, Sullivan S, and Klein S. Obesity and nonalcoholic fatty liver disease: biochemical, metabolic, and clinical implications. *Hepatology.* 2010;51(2):679-89.
4. Gancheva S, Jelenik T, Alvarez-Hernandez E, and Roden M. Interorgan Metabolic Crosstalk in Human Insulin Resistance. *Physiol Rev.* 2018;98(3):1371-415.
5. Hodson L. Hepatic fatty acid synthesis and partitioning: the effect of metabolic and nutritional state. *Proc Nutr Soc.* 2019;78(1):126-34.
6. Cusi K. Role of obesity and lipotoxicity in the development of nonalcoholic steatohepatitis: pathophysiology and clinical implications. *Gastroenterology.* 2012;142(4):711-25 e6.
7. Nakajima K, Nakano T, Tokita Y, Nagamine T, Inazu A, Kobayashi J, Mabuchi H, Stanhope KL, Havel PJ, Okazaki M, et al. Postprandial lipoprotein metabolism: VLDL vs chylomicrons. *Clin Chim Acta.* 2011;412(15-16):1306-18.
8. Cohen JC, Horton JD, and Hobbs HH. Human fatty liver disease: old questions and new insights. *Science.* 2011;332(6037):1519-23.
9. Farese RV, Jr., Zechner R, Newgard CB, and Walther TC. The problem of establishing relationships between hepatic steatosis and hepatic insulin resistance. *Cell Metab.* 2012;15(5):570-3.
10. Petersen KF, Dufour S, Befroy D, Lehrke M, Hendler RE, and Shulman GI. Reversal of nonalcoholic hepatic steatosis, hepatic insulin resistance, and hyperglycemia by moderate weight reduction in patients with type 2 diabetes. *Diabetes.* 2005;54(3):603-8.
11. Browning JD, and Horton JD. Molecular mediators of hepatic steatosis and liver injury. *J Clin Invest.* 2004;114(2):147-52.
12. Lichtenstein L, Berbee JF, van Dijk SJ, van Dijk KW, Bensadoun A, Kema IP, Voshol PJ, Muller M, Rensen PC, and Kersten S. Angptl4 upregulates cholesterol synthesis in liver via inhibition of LPL- and HL-dependent hepatic cholesterol uptake. *Arterioscler Thromb Vasc Biol.* 2007;27(11):2420-7.
13. Mandard S, Zandbergen F, van Straten E, Wahli W, Kuipers F, Muller M, and Kersten S. The fasting-induced adipose factor/angiopoietin-like protein 4 is physically associated with lipoproteins and governs plasma lipid levels and adiposity. *J Biol Chem.* 2006;281(2):934-44.
14. Kersten S, Mandard S, Tan NS, Escher P, Metzger D, Chambon P, Gonzalez FJ, Desvergne B, and Wahli W. Characterization of the fasting-induced adipose factor FIAF, a novel peroxisome proliferator-activated receptor target gene. *J Biol Chem.* 2000;275(37):28488-93.
15. Zhu P, Goh YY, Chin HF, Kersten S, and Tan NS. Angiopoietin-like 4: a decade of research. *Biosci Rep.* 2012;32(3):211-9.
16. Kristensen KK, Leth-Espensen KZ, Mertens HDT, Birrane G, Meiyappan M, Olivecrona G, Jorgensen TJD, Young SG, and Ploug M. Unfolding of monomeric lipoprotein lipase by ANGPTL4: Insight into the regulation of plasma triglyceride metabolism. *Proc Natl Acad Sci U S A.* 2020;117(8):4337-46.
17. Aryal B, Price NL, Suarez Y, and Fernandez-Hernando C. ANGPTL4 in Metabolic and Cardiovascular Disease. *Trends Mol Med.* 2019;25(8):723-34.

18. Kersten S. New insights into angiopoietin-like proteins in lipid metabolism and cardiovascular disease risk. *Curr Opin Lipidol.* 2019;30(3):205-11.
19. Dijk W, and Kersten S. Regulation of lipoprotein lipase by Angptl4. *Trends Endocrinol Metab.* 2014;25(3):146-55.
20. Desai U, Lee EC, Chung K, Gao C, Gay J, Key B, Hansen G, Machajewski D, Platt KA, Sands AT, et al. Lipid-lowering effects of anti-angiopoietin-like 4 antibody recapitulate the lipid phenotype found in angiopoietin-like 4 knockout mice. *Proc Natl Acad Sci U S A.* 2007;104(28):11766-71.
21. Gusarova V, O'Dushlaine C, Teslovich TM, Benotti PN, Mirshahi T, Gottesman O, Van Hout CV, Murray MF, Mahajan A, Nielsen JB, et al. Genetic inactivation of ANGPTL4 improves glucose homeostasis and is associated with reduced risk of diabetes. *Nat Commun.* 2018;9(1):2252.
22. Dewey FE, Gromada J, and Shuldiner AR. Variants in ANGPTL4 and the Risk of Coronary Artery Disease. *N Engl J Med.* 2016;375(23):2305-6.
23. Klarin D, Damrauer SM, Cho K, Sun YV, Teslovich TM, Honerlaw J, Gagnon DR, DuVall SL, Li J, Peloso GM, et al. Genetics of blood lipids among ~300,000 multi-ethnic participants of the Million Veteran Program. *Nat Genet.* 2018;50(11):1514-23.
24. Liu DJ, Peloso GM, Yu H, Butterworth AS, Wang X, Mahajan A, Saleheen D, Emdin C, Alam D, Alves AC, et al. Exome-wide association study of plasma lipids in >300,000 individuals. *Nat Genet.* 2017;49(12):1758-66.
25. Barja-Fernandez S, Moreno-Navarrete JM, Folgueira C, Xifra G, Sabater M, Castelao C, Fern OJ, Leis R, Dieguez C, Casanueva FF, et al. Plasma ANGPTL-4 is Associated with Obesity and Glucose Tolerance: Cross-Sectional and Longitudinal Findings. *Mol Nutr Food Res.* 2018;62(10):e1800060.
26. Lichtenstein L, Mattijssen F, de Wit NJ, Georgiadi A, Hooiveld GJ, van der Meer R, He Y, Qi L, Koster A, Tamsma JT, et al. Angptl4 protects against severe proinflammatory effects of saturated fat by inhibiting fatty acid uptake into mesenteric lymph node macrophages. *Cell Metab.* 2010;12(6):580-92.
27. Janssen AWF, Katiraei S, Bartosinska B, Eberhard D, Willems van Dijk K, and Kersten S. Loss of angiopoietin-like 4 (ANGPTL4) in mice with diet-induced obesity uncouples visceral obesity from glucose intolerance partly via the gut microbiota. *Diabetologia.* 2018.
28. Koster A, Chao YB, Mosior M, Ford A, Gonzalez-DeWhitt PA, Hale JE, Li D, Qiu Y, Fraser CC, Yang DD, et al. Transgenic angiopoietin-like (angptl)4 overexpression and targeted disruption of angptl4 and angptl3: regulation of triglyceride metabolism. *Endocrinology.* 2005;146(11):4943-50.
29. Xu A, Lam MC, Chan KW, Wang Y, Zhang J, Hoo RL, Xu JY, Chen B, Chow WS, Tso AW, et al. Angiopoietin-like protein 4 decreases blood glucose and improves glucose tolerance but induces hyperlipidemia and hepatic steatosis in mice. *Proc Natl Acad Sci U S A.* 2005;102(17):6086-91.
30. Wang Y, Liu LM, Wei L, Ye WW, Meng XY, Chen F, Xiao Q, Chen JY, and Zhou Y. Angiopoietin-like protein 4 improves glucose tolerance and insulin resistance but induces liver steatosis in high-fat-diet mice. *Mol Med Rep.* 2016;14(4):3293-300.
31. Aryal B, Rotllan N, Araldi E, Ramirez CM, He S, Chousterman BG, Fenn AM, Wanschel A, Madrigal-Matute J, Warrier N, et al. ANGPTL4 deficiency in haematopoietic cells promotes monocyte expansion and atherosclerosis progression. *Nat Commun.* 2016;7(12313.
32. Aryal B, Singh AK, Zhang X, Varela L, Rotllan N, Goedeke L, Chaube B, Camporez JP, Vatner DF, Horvath TL, et al. Absence of ANGPTL4 in adipose tissue improves glucose tolerance and attenuates atherogenesis. *JCI Insight.* 2018;3(6).

33. Spitler KM, Shetty SK, Cushing EM, Sylvers-Davie KL, and Davies BSJ. Regulation of plasma triglyceride partitioning by adipose-derived ANGPTL4 in mice. *Sci Rep.* 2021;11(1):7873.
34. Boren J, Taskinen MR, Olofsson SO, and Levin M. Ectopic lipid storage and insulin resistance: a harmful relationship. *J Intern Med.* 2013;274(1):25-40.
35. Petersen MC, and Shulman GI. Mechanisms of Insulin Action and Insulin Resistance. *Physiol Rev.* 2018;98(4):2133-223.
36. Stender S, Kozlitina J, Nordestgaard BG, Tybjaerg-Hansen A, Hobbs HH, and Cohen JC. Adiposity amplifies the genetic risk of fatty liver disease conferred by multiple loci. *Nat Genet.* 2017;49(6):842-7.
37. Sarwar R, Pierce N, and Koppe S. Obesity and nonalcoholic fatty liver disease: current perspectives. *Diabetes Metab Syndr Obes.* 2018;11(533-42.
38. Moshage H. Cytokines and the hepatic acute phase response. *J Pathol.* 1997;181(3):257-66.
39. Softic S, Cohen DE, and Kahn CR. Role of Dietary Fructose and Hepatic De Novo Lipogenesis in Fatty Liver Disease. *Dig Dis Sci.* 2016;61(5):1282-93.
40. Sinha RA, Singh BK, and Yen PM. Direct effects of thyroid hormones on hepatic lipid metabolism. *Nat Rev Endocrinol.* 2018;14(5):259-69.
41. Samovski D, Sun J, Pietka T, Gross RW, Eckel RH, Su X, Stahl PD, and Abumrad NA. Regulation of AMPK activation by CD36 links fatty acid uptake to beta-oxidation. *Diabetes.* 2015;64(2):353-9.
42. Kim HK, Youn BS, Shin MS, Namkoong C, Park KH, Baik JH, Kim JB, Park JY, Lee KU, Kim YB, et al. Hypothalamic Angptl4/Fiaf is a novel regulator of food intake and body weight. *Diabetes.* 2010;59(11):2772-80.
43. Steinberg GR, and Carling D. AMP-activated protein kinase: the current landscape for drug development. *Nat Rev Drug Discov.* 2019;18(7):527-51.
44. Liemburg-Apers DC, Willems PH, Koopman WJ, and Grefte S. Interactions between mitochondrial reactive oxygen species and cellular glucose metabolism. *Arch Toxicol.* 2015;89(8):1209-26.
45. Shafique E, Choy WC, Liu Y, Feng J, Cordeiro B, Lyra A, Arafah M, Yassin-Kassab A, Zanetti AV, Clements RT, et al. Oxidative stress improves coronary endothelial function through activation of the pro-survival kinase AMPK. *Aging (Albany NY).* 2013;5(7):515-30.
46. Schonfeld P, and Wojtczak L. Fatty acids as modulators of the cellular production of reactive oxygen species. *Free Radic Biol Med.* 2008;45(3):231-41.
47. Pike LS, Smift AL, Croteau NJ, Ferrick DA, and Wu M. Inhibition of fatty acid oxidation by etomoxir impairs NADPH production and increases reactive oxygen species resulting in ATP depletion and cell death in human glioblastoma cells. *Biochim Biophys Acta.* 2011;1807(6):726-34.
48. Dalle Pezze P, Ruf S, Sonntag AG, Langelaar-Makkinje M, Hall P, Heberle AM, Razquin Navas P, van Eunen K, Tolle RC, Schwarz JJ, et al. A systems study reveals concurrent activation of AMPK and mTOR by amino acids. *Nat Commun.* 2016;7(13254.
49. Li Y, Xu S, Mihaylova MM, Zheng B, Hou X, Jiang B, Park O, Luo Z, Lefai E, Shyy JY, et al. AMPK phosphorylates and inhibits SREBP activity to attenuate hepatic steatosis and atherosclerosis in diet-induced insulin-resistant mice. *Cell Metab.* 2011;13(4):376-88.
50. Bhandary B, Marahatta A, Kim HR, and Chae HJ. An involvement of oxidative stress in endoplasmic reticulum stress and its associated diseases. *Int J Mol Sci.* 2012;14(1):434-56.

51. Cnop M, Foufelle F, and Velloso LA. Endoplasmic reticulum stress, obesity and diabetes. *Trends Mol Med.* 2012;18(1):59-68.
52. Hummasti S, and Hotamisligil GS. Endoplasmic reticulum stress and inflammation in obesity and diabetes. *Circ Res.* 2010;107(5):579-91.
53. Prakash TP, Graham MJ, Yu J, Carty R, Low A, Chappell A, Schmidt K, Zhao C, Aghajan M, Murray HF, et al. Targeted delivery of antisense oligonucleotides to hepatocytes using triantennary N-acetyl galactosamine improves potency 10-fold in mice. *Nucleic Acids Res.* 2014;42(13):8796-807.
54. Mooradian AD. Dyslipidemia in type 2 diabetes mellitus. *Nat Clin Pract Endocrinol Metab.* 2009;5(3):150-9.
55. Do R, Willer CJ, Schmidt EM, Sengupta S, Gao C, Peloso GM, Gustafsson S, Kanoni S, Ganna A, Chen J, et al. Common variants associated with plasma triglycerides and risk for coronary artery disease. *Nat Genet.* 2013;45(11):1345-52.
56. Bailetti D, Bertoccini L, Mancina RM, Barchetta I, Capoccia D, Cossu E, Pujia A, Lenzi A, Leonetti F, Cavallo MG, et al. ANGPTL4 gene E40K variation protects against obesity-associated dyslipidemia in participants with obesity. *Obes Sci Pract.* 2019;5(1):83-90.
57. Barja-Fernandez S, Folgueira C, Castelao C, Pena-Leon V, Gonzalez-Saenz P, Vazquez-Cobela R, Aguilera CM, Gil-Campos M, Bueno G, Gil A, et al. ANGPTL-4 is Associated with Obesity and Lipid Profile in Children and Adolescents. *Nutrients.* 2019;11(6).
58. Oteng AB, Ruppert PMM, Boutens L, Dijk W, van Dierendonck X, Olivecrona G, Stienstra R, and Kersten S. Characterization of ANGPTL4 function in macrophages and adipocytes using Angptl4-knockout and Angptl4-hypomorphic mice. *J Lipid Res.* 2019;60(10):1741-54.
59. Gutgsell AR, Ghodge SV, Bowers AA, and Neher SB. Mapping the sites of the lipoprotein lipase (LPL)-angiopoietin-like protein 4 (ANGPTL4) interaction provides mechanistic insight into LPL inhibition. *J Biol Chem.* 2019;294(8):2678-89.
60. Havel RJ, and Hamilton RL. Hepatic catabolism of remnant lipoproteins: where the action is. *Arterioscler Thromb Vasc Biol.* 2004;24(2):213-5.
61. Brasaemle DL, Cornely-Moss K, and Bensadoun A. Hepatic lipase treatment of chylomicron remnants increases exposure of apolipoprotein E. *J Lipid Res.* 1993;34(3):455-65.
62. Toth PP. Triglyceride-rich lipoproteins as a causal factor for cardiovascular disease. *Vasc Health Risk Manag.* 2016;12(171-83.
63. Garcia D, Hellberg K, Chaix A, Wallace M, Herzig S, Badur MG, Lin T, Shokhirev MN, Pinto AFM, Ross DS, et al. Genetic Liver-Specific AMPK Activation Protects against Diet-Induced Obesity and NAFLD. *Cell Rep.* 2019;26(1):192-208 e6.
64. Foretz M, Even PC, and Viollet B. AMPK Activation Reduces Hepatic Lipid Content by Increasing Fat Oxidation In Vivo. *Int J Mol Sci.* 2018;19(9).
65. Watt MJ, Steinberg GR, Chen ZP, Kemp BE, and Febbraio MA. Fatty acids stimulate AMP-activated protein kinase and enhance fatty acid oxidation in L6 myotubes. *J Physiol.* 2006;574(Pt 1):139-47.
66. Clark H, Carling D, and Saggerson D. Covalent activation of heart AMP-activated protein kinase in response to physiological concentrations of long-chain fatty acids. *Eur J Biochem.* 2004;271(11):2215-24.
67. Hickson-Bick DL, Buja LM, and McMillin JB. Palmitate-mediated alterations in the fatty acid metabolism of rat neonatal cardiac myocytes. *J Mol Cell Cardiol.* 2000;32(3):511-9.
68. Schieber M, and Chandel NS. ROS function in redox signaling and oxidative stress. *Curr Biol.* 2014;24(10):R453-62.

FIGURES

Figure 1

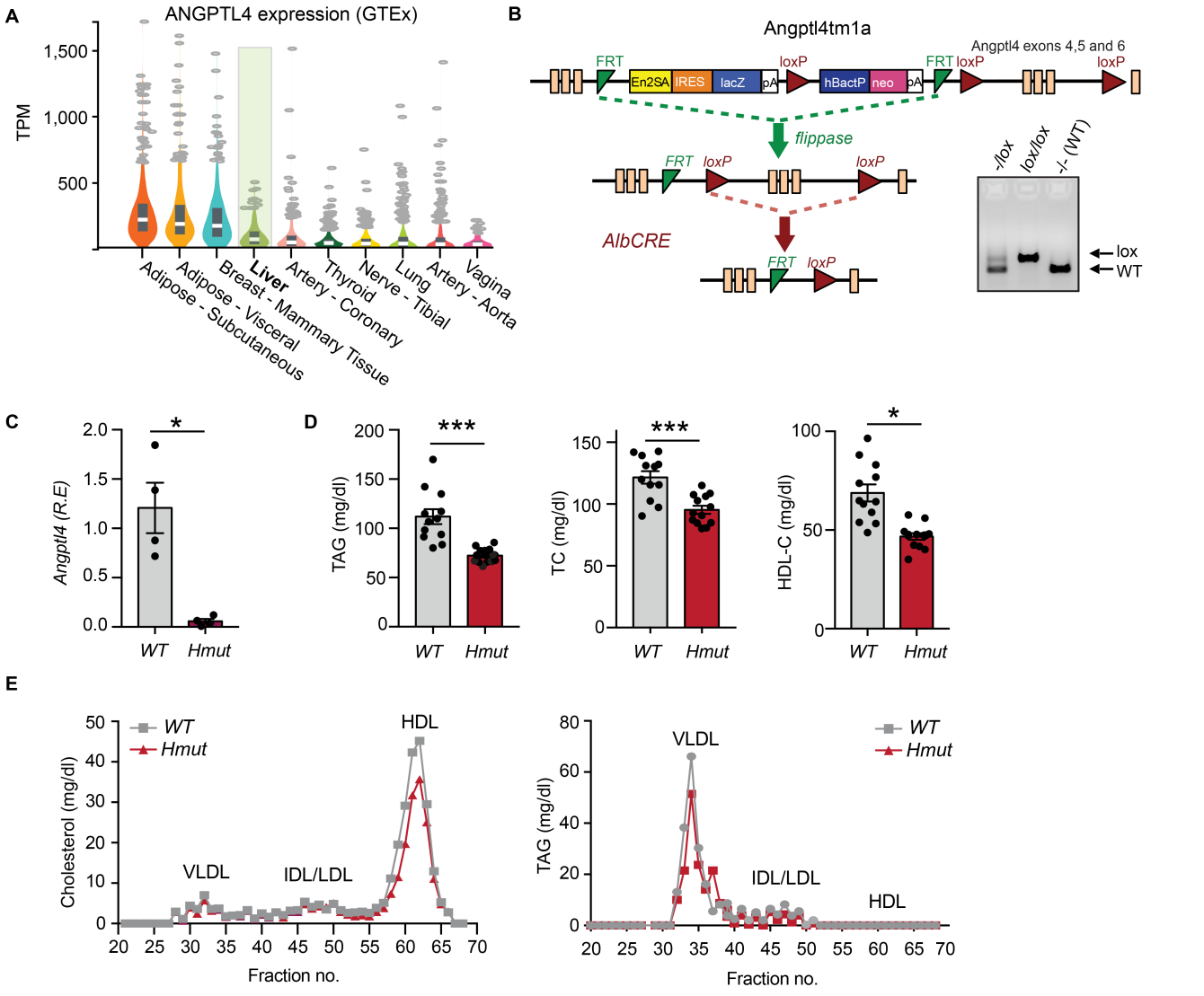

Figure 1. The loss of ANGPTL4 function in hepatocytes improves the serum lipid profile. (**A**) Analysis of human ANGPTL4 expression in different tissues using GTEx database. Liver is highlighted. TPM represents transcript per millions reads. (**B**) Schematic diagram illustrating the generation of hepatocyte-specific ANGPTL4 mutant (*Hmut*) mice. The construct is composed of a short flippase recombination enzyme (Flp)-recognition target (FRT), reporter, and a Cre recombinase recognition target (loxP). Angptl4 exons 4-6 are flanked by lox P site. Mice with the floxed allele were generated by crossing with flp recombinase-deleter mice (mid panel). Subsequently, these mice were bred with mice expressing Cre recombinase to produce tissue specific *Hmut* mice (bottom). PCR amplification of *Angptl4*$^{fl/fl}$ mice displaying bands from both, one, or none of the alleles floxed (Right panel). (**C**) mRNA expression of *Angptl4* in the liver of WT and *Hmut* mice. (**D**) Fasted plasma triacylglycerol (TAG; left panel), total cholesterol (middle panel), and HDL-C (right panel) from overnight fasted WT and *Hmut* mice chow diet (CD) for two months (n=10-13). (**E**) Cholesterol (left panel) and TAG (right panel) content of FPLC-fractionated lipoproteins from pooled plasma of overnight fasted WT and *Hmut* mice fed a CD for two months (n=7). R.E denotes relative expression. All data represent mean ± SEM. *p<0.05, ***p<0.001 comparing *Hmut* with WT mice using the unpaired t-test.

Figure 2

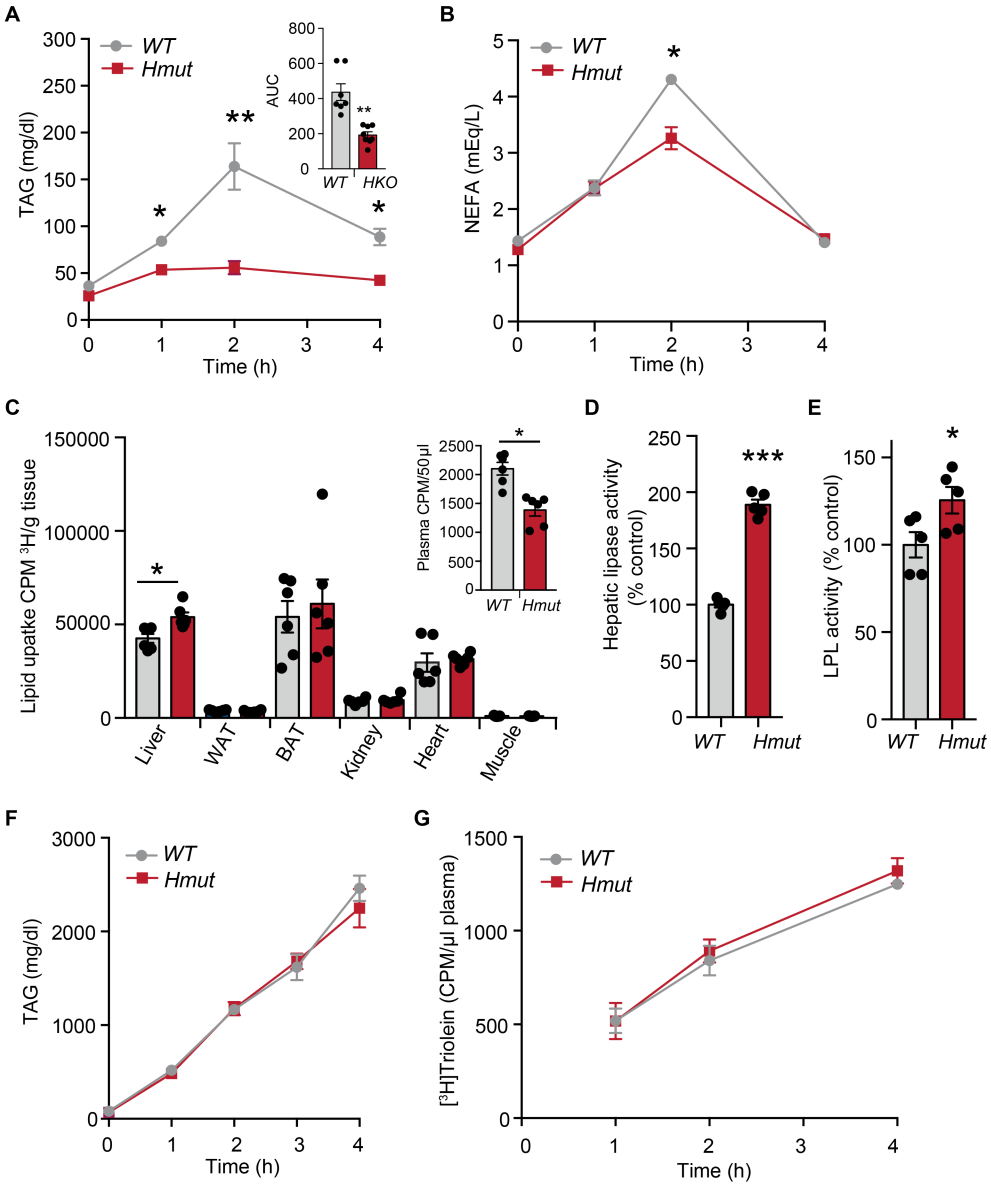

Figure 2. Inactivation of ANGPTL4 in hepatocytes enhances plasma TAG clearance and hepatic lipid uptake. (**A** and **B**) Oral lipid tolerance test showing the clearance of TAG and NEFA from the plasma of WT and *Hmut* mice fasted for 4h followed by oral gavage of olive oil. Inset represent the AUC. (**C**) Radioactivity incorporation in indicated tissues after 2h of oral gavage of [^{3}H]-labeled triolein in WT or *Hmut* mice fasted for 4h. Inset represent plasma lipid clearance. (**D** and **E**) HL and LPL activity in the post-heparin plasma from overnight fasted WT and *Hmut* mice. (**F**) Plasma TAG from overnight fasted WT and *Hmut* mice treated with plasma LPL inhibitor poloxamer 407 to inhibit the hydrolysis of circulating TAG (n=5). (**G**) Serum ^{3}H counts after injection of poloxamer 407 combined with oral lipid gavage containing ^{3}H-triolein (n=5). All data represent the mean ± SEM. *p<0.05 **p<0.01 ***p<0.001 comparing *Hmut* with WT mice using the unpaired t-test.

Figure 3

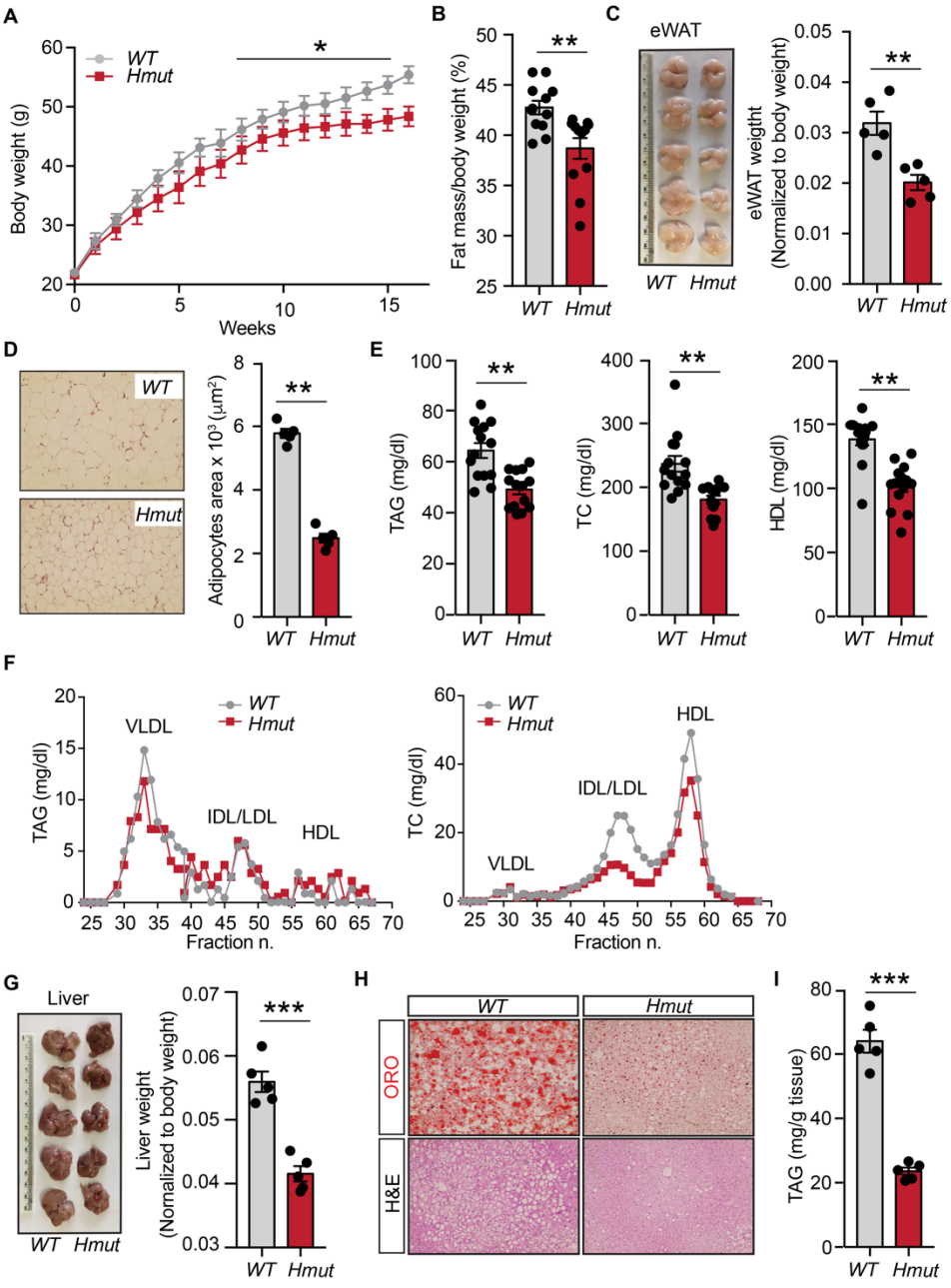

Figure 3. Hepatic ANGPTL4 deficiency protects from diet-induced obesity and decreases hepatic lipid accumulation. (**A** and **B**) Body weight and fat mass measured by Echo-MRI of WT and *Hmut* mice fed a high–fat diet (HFD) for 16 weeks. (n=10-13). (**C** and **D**) Fat (eWAT) weight and representative images of H&E sections of WAT and quantification of adipocyte size isolated from *WT* and *Hmut* mice fed an HFD for 16 weeks. Original magnification ×10; (**E**) Levels of TAG, total cholesterol (TC), and HDL-C in the plasma of overnight fasted WT and *Hmut* mice fed an HFD for 16 weeks. (**F**) FPLC analysis of lipoprotein profile from pooled plasma of overnight fasted WT and *Hmut* mice (n=5). (**G-I**) Representative images of the liver, Liver weight (G), representative pictures of Oil Red O and H&E-stained sections of liver isolated from WT and *Hmut* mice fed HFD for 16 weeks (**H**) and hepatic TAG levels (**I**). Original magnification ×20; All data represent the mean ± SEM. *p<0.05 **p<0.01 ***p<0.001 comparing *Hmut* with WT mice using the unpaired t-test.

Figure 4

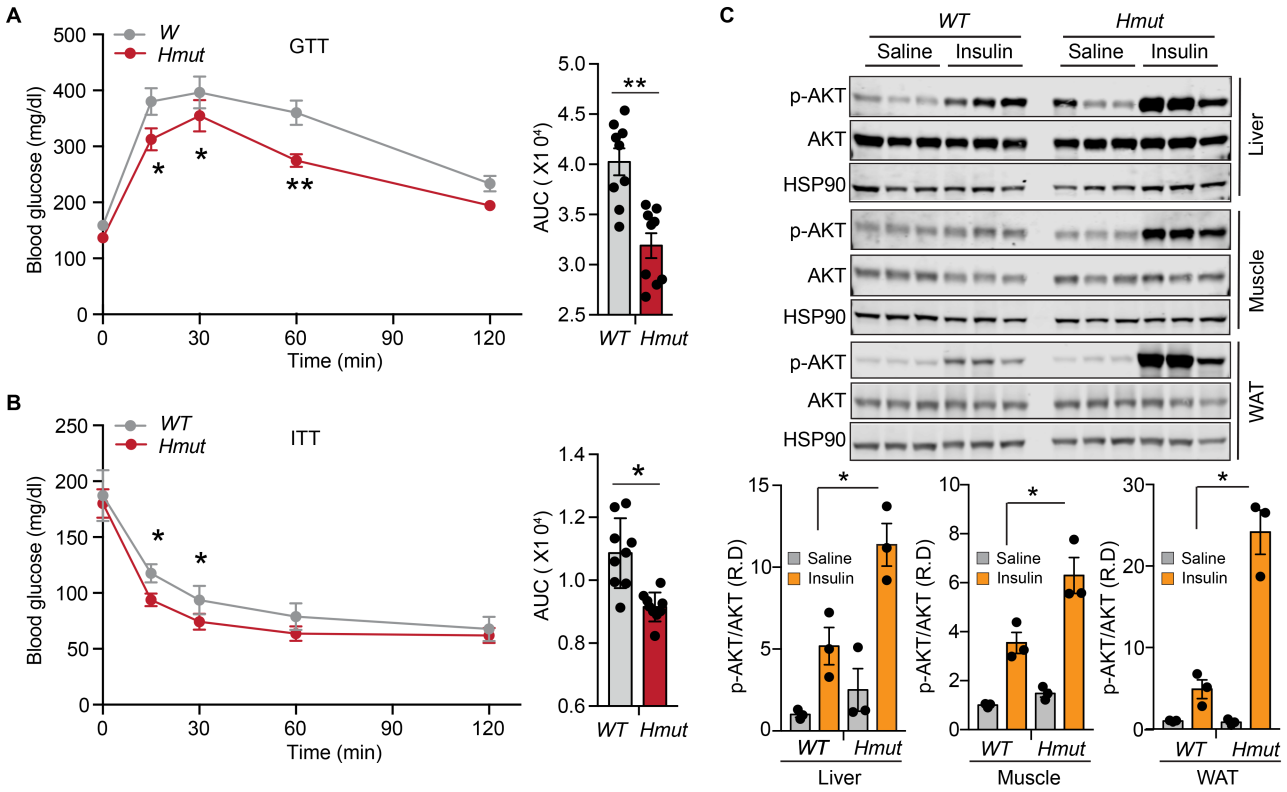

Figure 4. Lack of ANGPTL4 function in hepatocytes exhibits improved glucose homeostasis and enhanced insulin sensitivity. (**A**) Intraperitoneal glucose (1 g/kg body weight) tolerance test (GTT) and area under the curve (right panels) of mice fed an HFD for 16 weeks. (**B**) Intraperitoneal insulin (2.0 U/kg body weight) tolerance test (ITT) and area under the curve (right panels) of mice fed an HFD for 16 weeks. (**C**) Representative immunoblot images and quantification of Akt (Ser 473 phosphorylation status relative to total AKT (right panels) in the liver, muscle, and adipose tissue, 15 min after an intraperitoneal bolus of insulin (2.0 U/kg) or saline in 16 weeks HFD fed WT vs. *Hmut* mice. R.D denotes relative density. All data represent mean ± SEM. *p<0.05 **p<0.01 comparing *Hmut* with *WT* mice using the unpaired t-test.

Figure 5

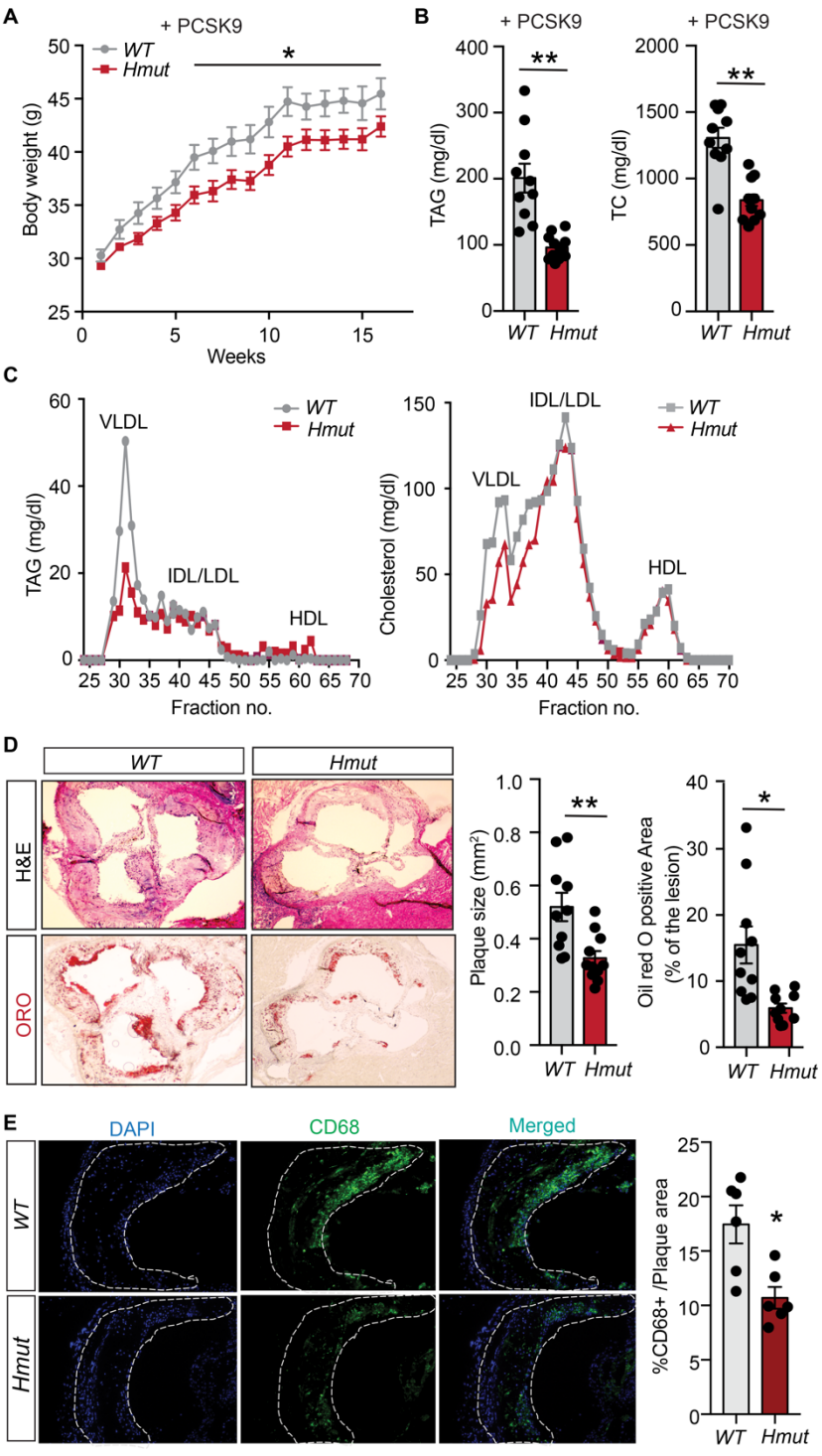

Figure 5. Genetic loss of ANGPTL4 in hepatocytes improves obesity and attenuates atherosclerosis. (**A**) Body weight (**B**), Plasma triacylglycerides (TAG), and total cholesterol (TC) from overnight fasted *WT* and *Hmut* mice fed a western-type diet (WD) for 16 weeks. (**C**) Lipoprotein profile analysis of pooled plasma of overnight fasted *WT* and *Hmut* mice (n=5). (**D**) Left: representative histological analysis of a cross-section of the aortic root sinus isolated from WT and *Hmut* mice fed a WD for 16 weeks stained with H&E (upper panels) and Oil red O (ORO; lower panels). Right: quantification of plaques size and the percentage area of neutral lipid accumulation calculated from H&E or ORO cross-sections, respectively. Original magnification ×10; (**E**) Representative cross-section analysis of macrophage content (CD68-positive cells) of the aortic root from WT and *Hmut* mice fed a WD for 16 weeks. Quantifications of the graphs on the right. Original magnification ×10. All data represent mean ± SEM. *p<0.05, **p<0.01 comparing *Hmut* with WT mice using the unpaired t-test.

Figure 6

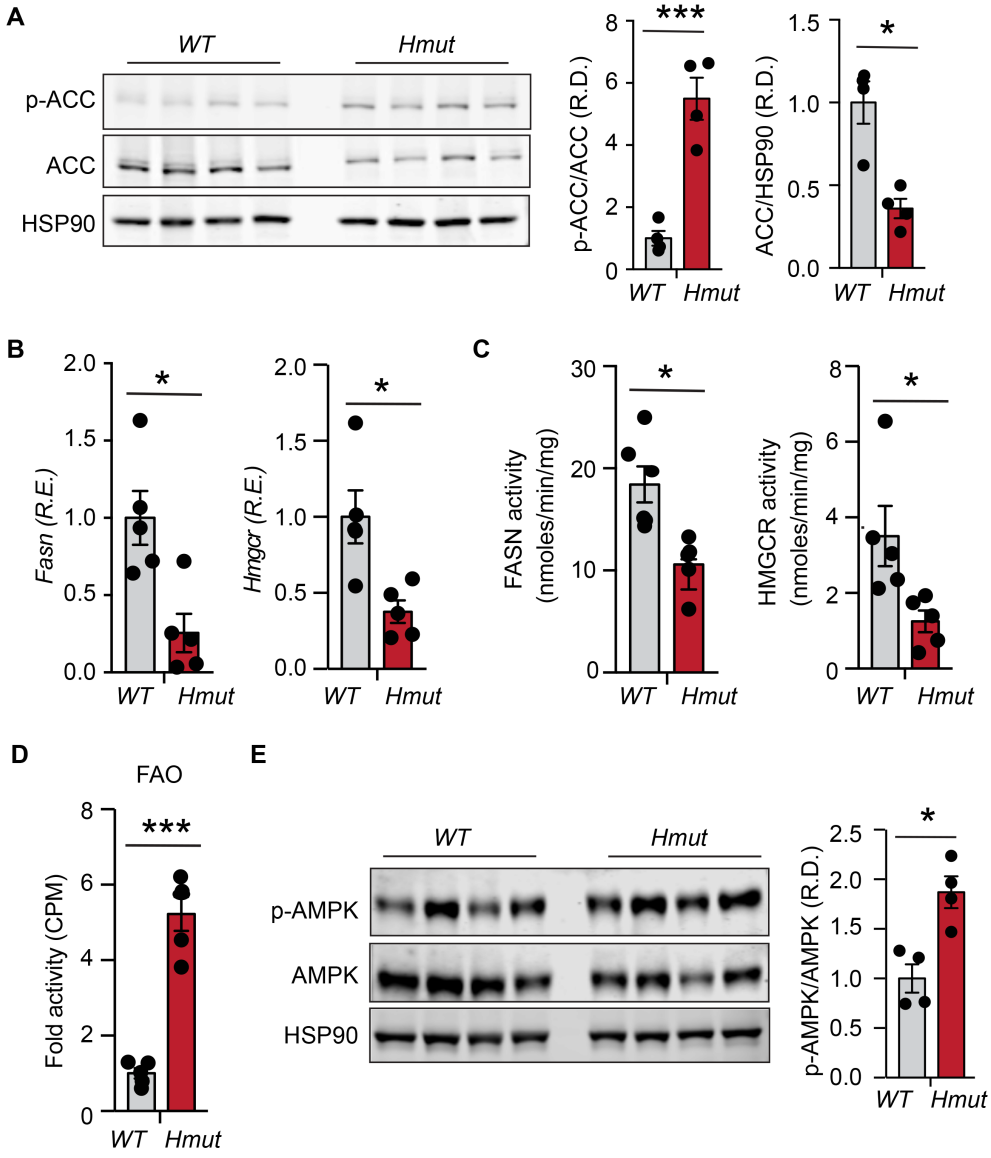

Figure 6. Loss of ANGPTL4 in hepatocytes inhibits DNL pathway and promotes FAO. (**A**) Representative immunoblot images showing p-ACC and ACC levels in the liver isolated from fasted WT and *Hmut* mice fed a chow diet (CD) for eight weeks. The right panel shows p-ACC/ACC & ACC/HSP90 ratios from immunoblot images quantification. (**B**-**D**) Expression and the respective activity of the enzymes FASN and HMGCR and FAO in the liver isolated from fasted mice. (**E**) Immunoblot images of p-AMPK and total AMPK protein in the liver isolated from fasted mice. Densitometric analysis shown in the right panels. R.E denotes relative expression and R.D denotes relative density respectively. All data represent the mean ± SEM. *p<0.05 ***p<0.001 comparing *Hmut* with WT mice using the unpaired t-test.

Figure 7

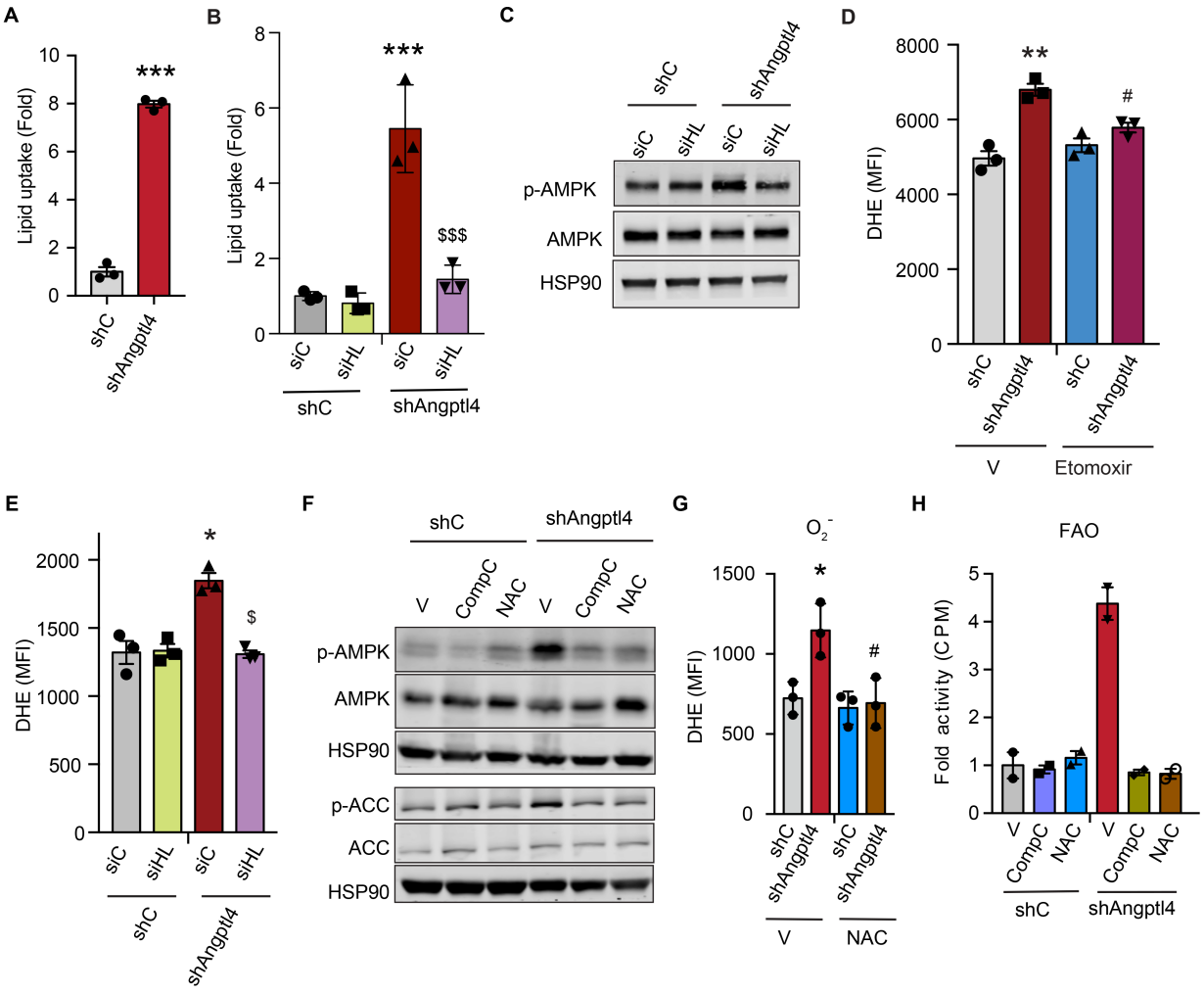

Figure 7. Inhibition of ROS and AMPK in HepG2 cells abrogates the effect of ANGPTL4 in lipid metabolism. (**A** and **B**) HepG2 cells were stably transfected with 3 different shRNAs against *ANGPTL4* and HL expression was transiently suppressed transfecting cells with specific siRNAs. HepG2–shC or HepG2-shAngptl4 cells transfected with HL or non-silencing (NS) siRNAs were treated with radiolabeled chylomicron for 2h. Graph shows lipid uptake as a fold change of control (shC). (**C**) Representative immunoblot images showing the levels of p-AMPK, AMPK, and HSP90 in HepG2-shC and HepG2-sh shAngptl4 cells transfected with HL or non-silencing (NS) siRNAs grown under the similar conditions mentioned in (**B**) (**D**) Relative ROS level in HepG2-shC and HepG2-shNAGPTL4 cells treated with either DMSO or Etomoxir (40μM) for 12h. (**E**) Relative ROS generation in cells used in (**B** and **C**). (**F**) Representative immunoblot images showing the levels of p-AMPK, AMPK, pACC, ACC and HSP90 in HepG2-shC and HepG2-shNAGPTL4 cells treated with or without compound C (20μM or NAC (5mM) for 24h. (**G**) Relative ROS level in the HepG2-shC and HepG2-shNAGPTL4 cells treated with or without NAC (5mM) for 24h. (**H**) FAO in cells under the condition mentioned in (**F**). MFI denotes mean fluorescence intensity. All data represent mean ± SEM. *,$,#p<0.05, **,$$,##p<0.01, ***p<0.001 as determined by two way ANOVA followed by Bonferroni posttest analysis (* represent comparison between HepG2-shANGPTL4 and HepG2-shC while # and $ represent comparison between HepG2-shANGPTL4 –vehicle ctrl vs HepG2-shANGPTL4-CompC and HepG2-shANGPTL4 –vehicle ctrl vs HepG2-shANGPTL4 -NAC respectively).

Figure 8

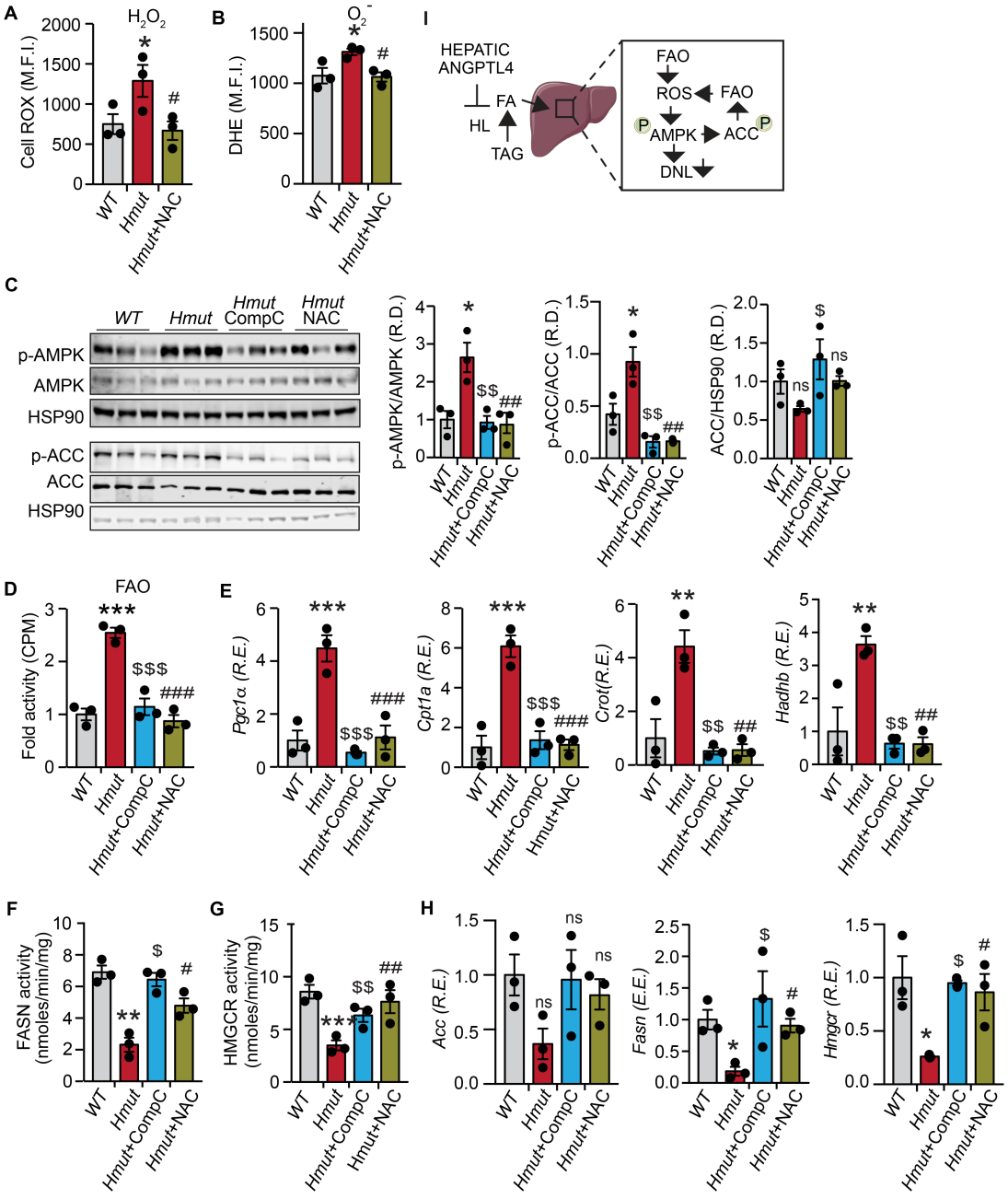

Figure 8. Inhibition of ROS dependent activation of AMPK in *Hmut* mice reverses the hepatic lipid metabolism. Eight weeks old *Hmut* mice were divided randomly into three groups. Each group of mice was administered with vehicle control (V), compound C (CompC), and NAC, respectively, for the three consecutive days. (**A** and **B**) Determination of cellular ROS (H_2O_2 and O_2^-) in the hepatocytes isolated from the *Hmut* mice with indicated treatment groups. (**C**) Immunoblots showing the levels of p-AMPK, AMPK, p-ACC, and ACC in the liver isolated from fasted *Hmut* mice from the indicated treatment groups. The right panel shows image quantification of p-AMPK/AMPK, p-ACC/ACC, and ACC/HSP90 ratios from immunoblot densitometry. (**D**) FAO in the liver of fasted *Hmut* mice from indicated treatment groups. (**E**) mRNA expression profile of FAO genes (**F** and **G**) FASN and HMGCR enzymatic activity in the liver. (**H**) FA biosynthesis genes in the liver of the mice administered with indicated inhibitors, as accessed by qRT-PCR. (**I**) Proposed mechanism for the role of liver-derived ANGPTL4 in hepatic lipid metabolism. R.E denotes relative expression and R.D denotes relative density respectively. All data represent mean ± SEM. *,$,#p<0.05, **,$$,##p<0.01, ***,$$$,###p<0.001 as determined by one way ANOVA followed by Bonferroni posttest analysis (* represent comparison between WT and *Hmut* mice while # and $ represent comparison between *Hmut*-ctrl vs *Hmut*-CompC and *Hmut*-ctrl vs *Hmut*-NAC respectively).

Figure 9

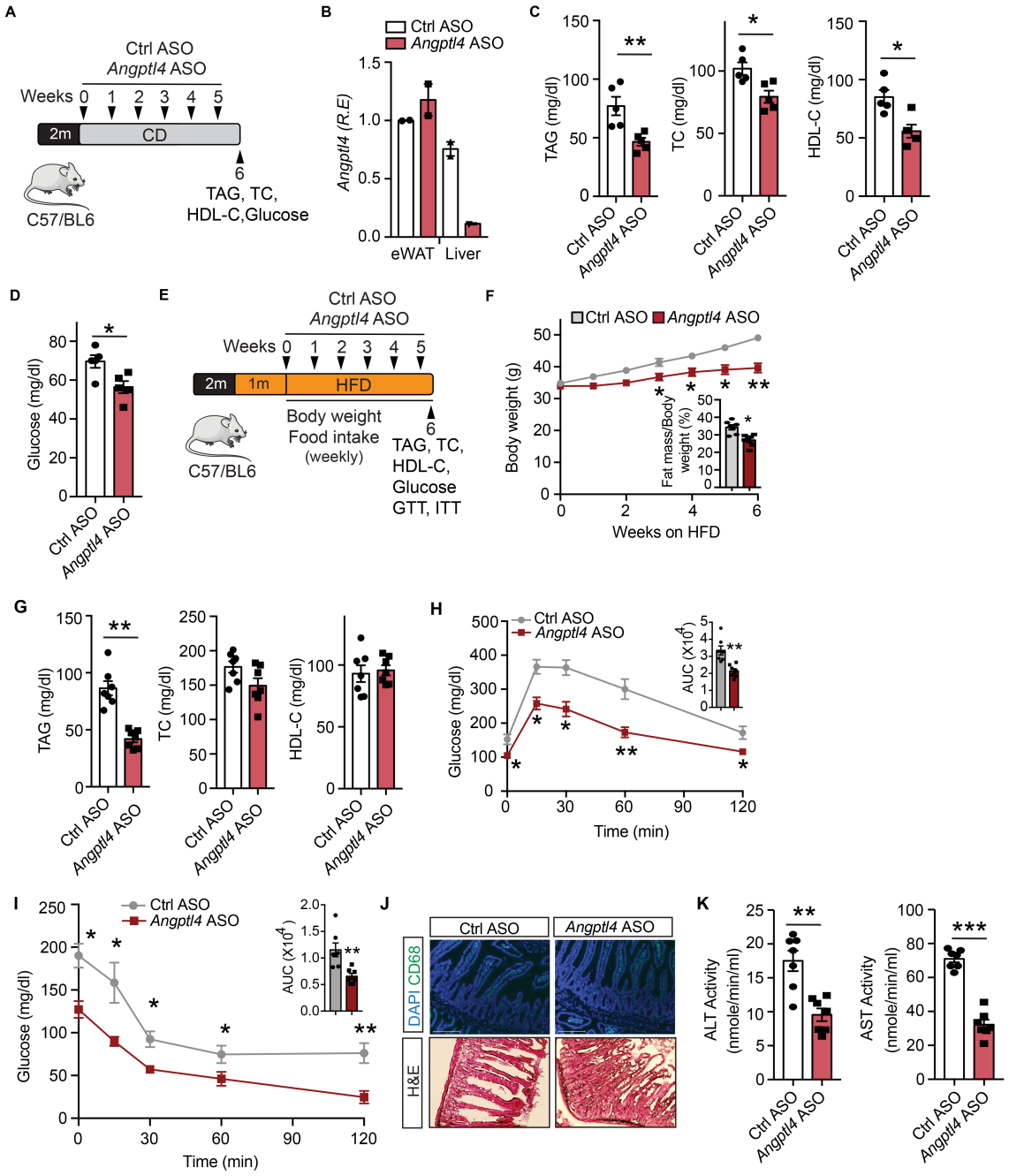

Figure 9. GalNac-conjugated ANGPTL4-ASO treatment improves whole body metabolism in physiological and pathophysiological conditions. (**A**) Schematic presentation of the experimental design of GalNac-conjugated ANGPTL4-ASO (ANGPTL4 ASO) treatment of chow diet (CD) fed mice. (**B**) *Angptl4* expression in eWAT and liver. (**C**) Plasma TAG, TC and HDL-C from overnight fasted 6 weeks *Angptl4* ASO or Ctrl-ASO treated WT mice. (**D**) Fasting blood glucose (**E**) The strategy for the treatment of GalNac-conjugated ANGPTL4 ASO in fat-induced obese mice. HFD fed mice were treated with *Angptl4*-ASO or Ctrl-ASO for 6 weeks. (**F**) Body weight: the number of weeks on a HFD diet is indicated (The treatment was started at week 5 of HFD feeding). Inset represent the fat mass measured by Echo-MRI. (**G**) Plasma TAG, TC and HDL-C from overnight fasted 6 weeks ANGPTL4 ASO or Ctrl ASO treated HFD fed WT mice. (**H** and **I**) Intraperitoneal glucose tolerance test (GTT) and Intraperitoneal insulin tolerance test (ITT) in six weeks ANGPTL4 ASO or Ctrl ASO injected in mice fed a HFD. Inset represents the AUC. (**J**) Representative images of small intestine cross-sections of HFD fed mice from the 10-weeks treatment of *Angptl4* ASO or Ctrl ASO were stained with macrophage marker CD68 and H&E. Original magnification ×20. (**K**) The activity of plasma ALT and AST after 10-weeks treatment of ANGPTL4 ASO or Ctrl ASO in HFD-induced obese mice. All data represent mean ± SEM. *p<0.05, **p<0.01, ***p<0.001 comparing *Angptl4* ASO with Ctrl ASO treated mice using the unpaired t-test.

Figure 10

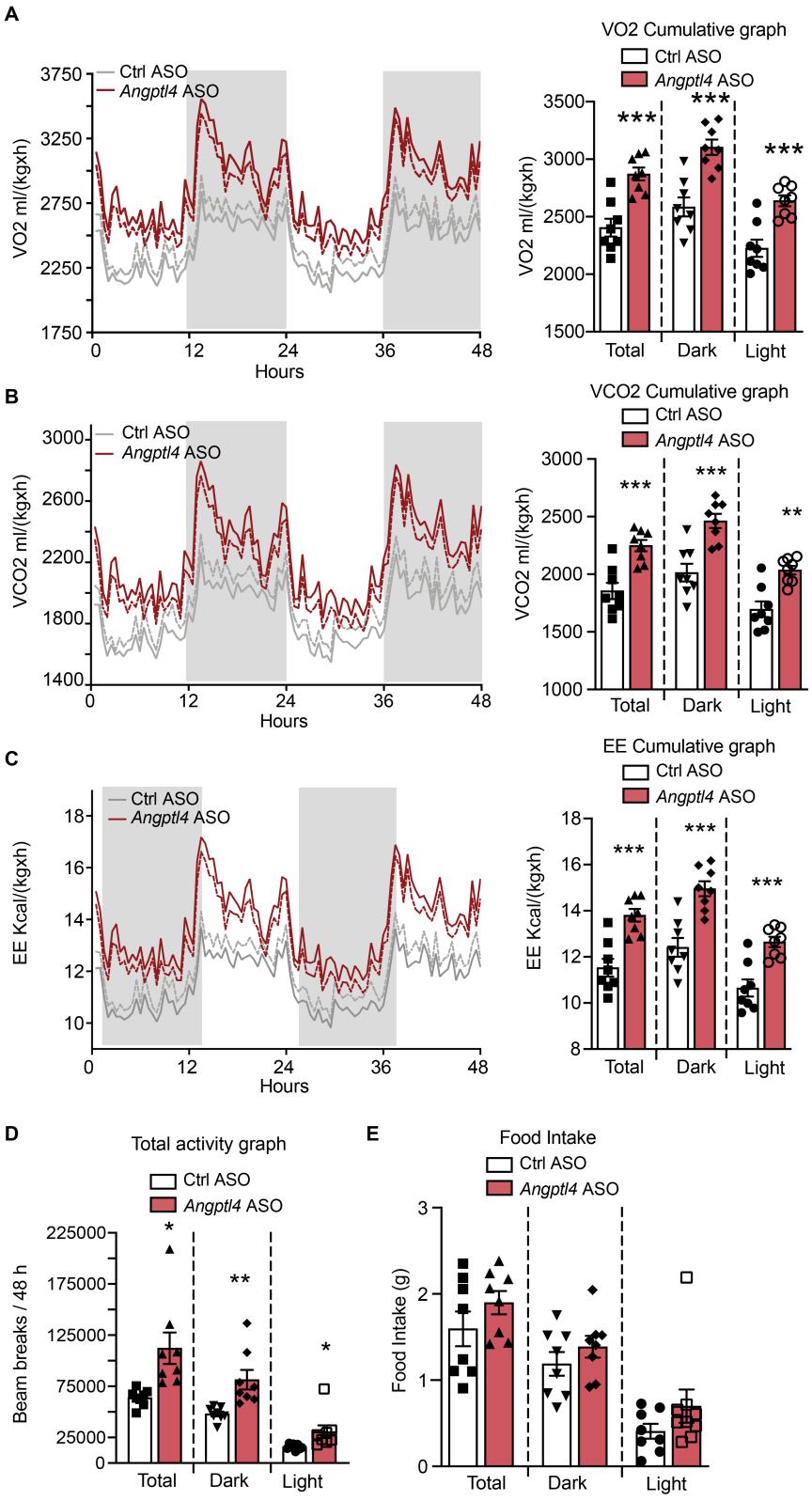

Figure 10. Suppression of hepatocyte *Angptl4* by GalNac-conjugated *Angptl4* ASO increases Energy expenditure without influencing food intake. (**A-E**) Metabolic analysis of *Angptl4* ASO and control ASO treated HFD fed mice over a 48 h period. (**A**) Oxygen consumption. The right panel shows cumulative graph of O_2 consumption. **(B)** Carbon dioxide production. Cumulative graph on the right. (**C**) Energy expenditure. The right section indicates cumulative graph. (**D**) Total activity. (**E**) Food consumption. All data represent mean ± SEM. *p<0.05, **p<0.01, ***p<0.001 comparing *Angptl4* ASO with Ctrl ASO treated mice using an unpaired t-test.